

High Resolution Gamma-Ray Spectroscopy and the Fascinating Angular Momentum Realm of the Atomic Nucleus

M. A. Riley¹ *

Department of Physics, Florida State University, Tallahassee, FL 32306, USA

J. Simpson² †

STFC Daresbury Laboratory, Daresbury, Warrington, WA4 4AD, UK

E. S. Paul³ ‡

Department of Physics, University of Liverpool, Liverpool, L69 7ZE, UK

PACS REF: 21.10.Re, 21.10.Tg, 27.70.+q, 29.30.Kv

Abstract

In 1974, Aage Bohr and Ben Mottelson, predicted the different “phases” that may be expected in deformed nuclei as a function of increasing angular momentum and excitation energy all the way up to the fission limit. While admitting their picture was highly conjectural they confidently stated “...with the ingenious experimental approaches that are being developed, we may look forward with excitement to the detailed spectroscopic studies that will illuminate the behaviour of the spinning quantized nucleus”. High resolution gamma-ray spectroscopy has indeed been a major tool in studying the structure of atomic nuclei and has witnessed numerous significant advances over the last four decades. This article will select highlights from investigations at the Niels Bohr Institute and Daresbury Laboratory in the late 1970’s and early 1980’s some of which have continued to the present day, to illustrate the remarkable diversity of phenomena and symmetries exhibited by nuclei in the angular momentum - excitation energy plane that continue to surprise and fascinate scientists.

1. Introduction to gamma spectroscopy and arrays

Gamma-ray spectroscopy plays a pivotal role in our investigations into the properties and behaviour of the strongly interacting aggregation of fermions that is called the atomic nucleus. The study of the gamma-ray emissions from excited nuclei reveal a rich system that displays a wealth of dynamical and static facets [1]. The number of nucleons is finite but still sufficient (≤ 300) to allow correlations. Thus nuclei exhibit a variety of collective properties yet are simple enough to display the single-particle basis of these collective effects and also single-particle properties. The diversity of symmetries and phenomena exhibited by nuclei is remarkable and continues to fascinate and surprise scientists as the development of increasingly sensitive instruments along with new accelerator developments continually reveals unexpected properties. This article will select highlights from the last four decades from high-spin investigations at the Niels Bohr

Institute in Denmark and Daresbury Laboratory in the UK (see Fig. 1 and Ref. [2]) in the late 1970’s and early 1980’s, which are associated with the development of large escape-suppressed Ge arrays, to the present day.

A fundamental quest in nuclear structure physics is to explore the behaviour of nuclei at the limits of angular momentum and excitation energy. The studies give us deep insight into the many body nuclear problem and especially the role of the “intruder” orbitals that help define the magic numbers and which play a dominant part in determining the properties (shapes, moments of inertia, pairing correlations, collectivity, etc.) of nuclei at high spin. In fact, it was as early as 1937 that Niels Bohr and Fritz Kalckar [3] proposed that one could learn about the evolving structure and shape of excited nuclei by detecting their gamma-ray emissions. This is similar to investigating atomic or molecular structure by the radiation emitted when these systems are excited. Indeed, novel detector technologies continue to revolutionise gamma-ray spectroscopic studies and our understanding of the atomic nucleus. For example, as shown in Fig. 2, the discoveries in Erbium-158 (^{158}Er : $Z = 68$, $N = 90$) have benefited enormously from the progress in detector technology. The next major technological step is to move towards a 4π Ge detector ball using gamma-ray energy tracking technology, see below. This will bring yet another revolution to the field of gamma-ray spectroscopy and usher in a new era in nuclear structure physics.

1.1. Spectrometer developments

Each major advance in gamma-ray detector technology has resulted in significant new phenomena being discovered bringing fresh insight into the structure of nuclei. At present the field is transitioning from the “Gamma-Sphere’s” or large 4π arrays of escape-suppressed spectrometers, such as Gammasphere and Euroball, to 4π Ge shell arrays, such as GRETA (Gamma Ray Energy Tracking Array) in the USA and AGATA (Advanced Gamma Tracking Array) in Europe, see Ref. [4, 5] and references therein. These latter systems will employ the technique of gamma-ray tracking in electrically segmented Ge crystals

*e-mail: mriley@physics.fsu.edu

†e-mail: john.simpson@stfc.ac.uk

‡e-mail: esp@ns.ph.liv.ac.uk



Fig. 1: The Nuclear Structure Facility [2] at Daresbury Laboratory in the UK which began operations in 1983 and enjoyed a period of intense activity where many significant discoveries were made, some of which are featured in this article, until its untimely closing in 1993.

abandoning the concept of physical suppression shields. The first step towards the implementation of these 4π Ge arrays are the 1π systems, AGATA in Europe (initial phase) and GRETINA (Gamma Ray Energy Tracking In beam Nuclear Array) in the USA, which have been recently constructed and have completed their initial physics campaigns.

Physics highlights and technical details of many of these developments in Ge based detector systems can be found in Refs. [6, 7, 8]. Developments and highlights from the previous two decades are contained in Refs. [9, 10]. The different era's or time periods for each significant technical advance are illustrated in Fig. 2. A classic example of the evolution of gamma-ray detector systems through the decades, which demonstrates our ability to observe new physical phenomena, comes from the study of the yrast (lowest energy state for a given angular momentum) states in the rare-earth nucleus, ^{158}Er , (see also Refs [11, 12, 13] and references therein). In addition, Fig. 3 illustrates similar progress in other nuclei, for example ^{156}Dy , by showing the evolution of spectra of the yrast band sequence through the decades [14, 15, 16, 17, 18].

In the early 1960's attempts to measure the evolution of nuclear structure with angular momentum and excitation energy via gamma-ray spectroscopy were made with a few NaI(Tl) scintillation detectors. The sensitivity of such experiments was limited both by the poor resolution of the scintillation detectors (about 90 keV at 1300 keV) as well as by the small number and size of the detectors. Nevertheless, such early experiments were able to establish the low spin ($I \sim 6 - 10\hbar$) rotational structure of nuclei [14], see Fig. 3.

A major step forward came with the development of reverse biased germanium detectors in the mid 1960s. Germanium (either Ge(Li) or hyperpure-Ge) detectors [19, 20, 21] have very good energy resolution, ranging from ~ 1 keV at 122 keV to ~ 2 keV at 1332 keV. The initial advance in the spectroscopy of high-spin states was taken at the Niels Bohr Institute in the late 1970s when sev-

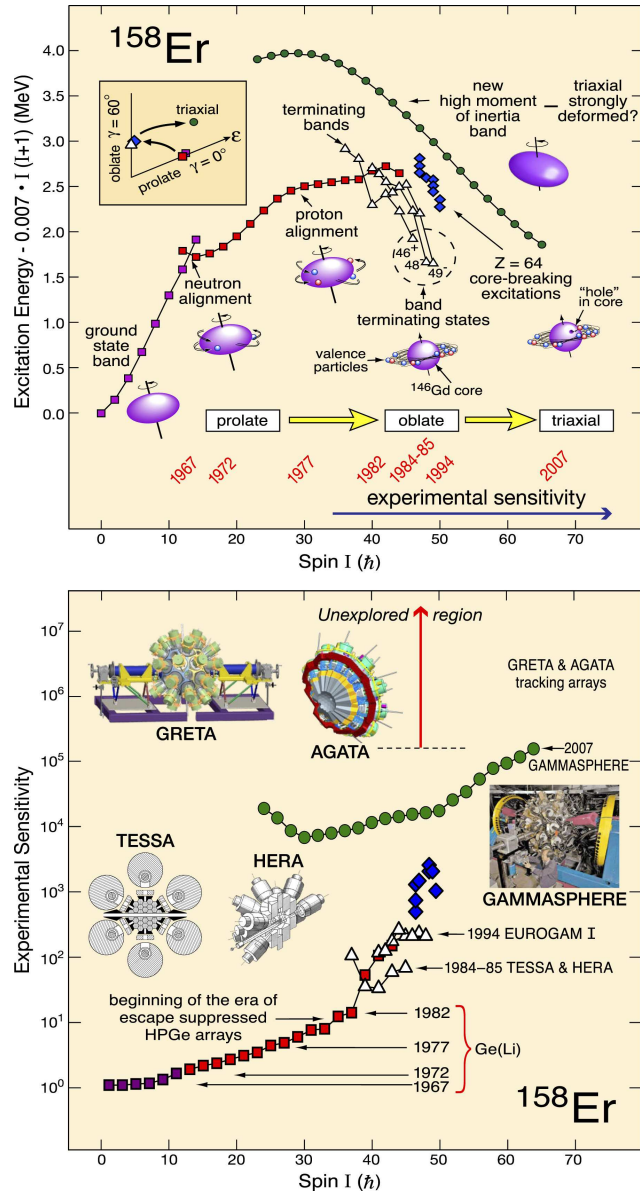


Fig. 2: Top: the evolution of nuclear structure in ^{158}Er with angular momentum (spin) and excitation energy. The inset shows the changing shape of ^{158}Er with increasing spin within the standard (ϵ , γ) deformation plane. The parameters ϵ and γ represent the eccentricity from sphericity and triaxiality, respectively. Bottom: the experimental sensitivity of detection (proportional to the inverse of the observed gamma-ray intensity) is plotted as a function of spin showing the development of gamma-ray detector technology with time that are associated with nuclear structure phenomena in ^{158}Er . "TESSA", "HERA", "EUROGAM I", "GAMMASPHERE", "GRETA", and "AGATA" are the names of specific gamma-ray detector arrays.

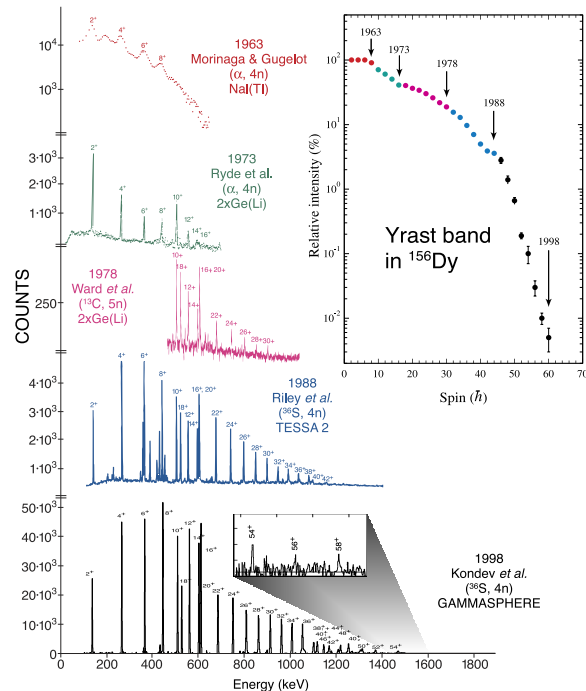


Fig. 3: Spectra showing the evolution of the yrast band in ^{156}Dy through the decades [14, 15, 16, 17, 18]. The top insert illustrates the observation of weaker and more exotic gamma-ray signals with increasing angular momentum through the decades.

eral Ge(Li) detectors were used in an array. Indeed, using just two Ge(Li) detectors the phenomenon of backbending (spin $\sim 15\hbar$) was discovered by Johnson et al. [22] and using four detectors Riedinger et al. [23] established the detailed quasiparticle structure [24, 25] of $^{160,161}\text{Yb}$ up to spin $30\hbar$.

Although these early experiments provided exceptional results, a major experimental problem remained; namely, that of a poor peak-to-background ratio caused by incomplete energy collection in the Ge detector. This problem is common to all experiments using bare Ge detectors.

It was realized that if the Ge detectors are surrounded by a dense scintillator (bismuth germanate (BGO) being the most common), which detects gamma rays that Compton scatter or escape out of the Ge crystal, a much better ratio of full-energy to total recorded events (called the peak-to-total, or P/T ratio) was achieved. The detection of gamma rays in the shield scintillator triggered the electronics system to suppress or reject the partial-energy pulse in the Ge detector. This improves the Peak to Total ratio for a 1.3 MeV gamma ray from about 0.28 for the bare crystal to about 0.6, see Fig. 4. This is an enormously important signal to background improvement, which makes practical the collection of high-fold coincidence data. For example, for a typical situation when six gamma rays hit separate Ge detectors in the Gammasphere spectrometer [26, 27], with escape-suppression,

the fraction of full-energy photo-peaks events increases by a factor of about 100. For increase in both efficiency and granularity, escape-suppressed detectors are assembled into arrays. The first such array, called TESSA (The Escape Suppressed Spectrometer Array) was set up at the Niels Bohr Institute in 1980 and consisted of five Ge(Li) detectors surrounded by NaI(Tl) shields.

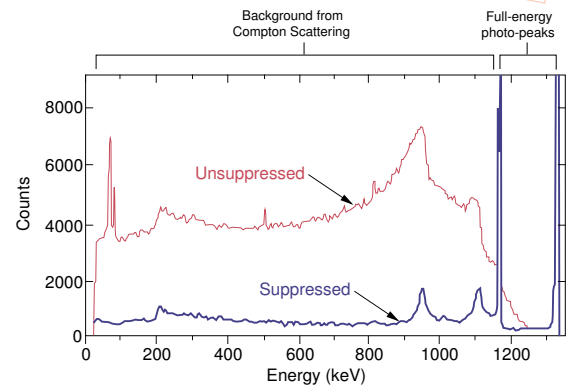


Fig. 4: (Top) Modern escape-suppressed spectrometer array schematic [28]. (Bottom) Unsuppressed and suppressed spectra for ^{60}Co showing the major gain in peak to background performance from the use of escape suppression. The full energy photo-peaks have been normalized in the two spectra.

The escape suppressed spectrometer arrays led to a revolution in gamma-ray spectroscopy. This revolution was sparked when Barna Nyako, a visitor from Debrecen, was setting gates on the weak intensity low-deformation band in ^{152}Dy [31] in the control room at Daresbury Laboratory and came across a remarkable sequence of 19 coincident gamma rays of even lower intensity. The authors were privileged enough to be among the first handful of people that Barna shared this momentous discovery with. This was very exciting indeed but we were sworn to secrecy! In May 1986 Peter Twin revealed the discrete superdeformed band in ^{152}Dy [32] for the first time to a general audience at the workshop on nuclear structure at the Niels Bohr Institute, see Fig. 5. The spectrum was met with a round

of applause from a jam packed auditorium, with Ben and Aage also joining in the celebration which everyone understood marked a new era in nuclear structure physics. However, Ben and Aage had been shown the game changing spectrum in a private meeting with the Daresbury-Liverpool-NBI collaboration just before the public unveiling, which we can all agree was the noble thing to do!

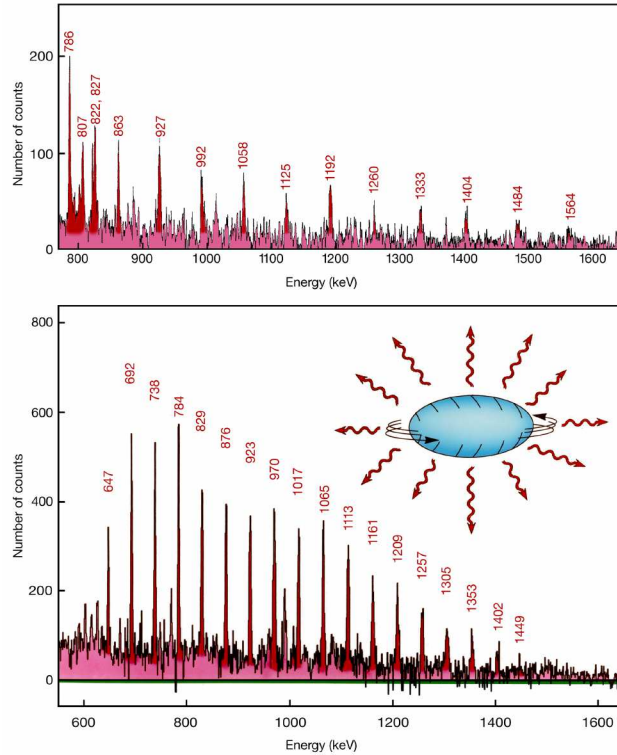


Fig. 5: The original high-spin superdeformed bands in (top) ^{132}Ce [33] and (bottom) ^{152}Dy [32] discovered at Daresbury Laboratory with TESSA2 and TESSA3, respectively. Such regularity was previously unknown in nuclear physics and led to superdeformed nuclei often being referred to as “nuclear pulsars”. It was not until 2002, using Gammasphere [34], that single-step direct links from the superdeformed band to the yrast line was determined thus fixing the excitation energy and spin of the ^{152}Dy band. However, the superdeformed yrast band in ^{132}Ce has resisted attempts to be linked in a similar manner in experiments using both Euroball and Gammasphere, indicating that the decay out of the second well is perhaps much more fragmented in this case.

Escape suppression technology that started with TESSA was the basis for many arrays worldwide with Gammasphere being one of the latest with BGO shields surrounding up to 110 Ge crystals, see Fig. 6.

The period between TESSA and Gammasphere saw many advances in detector array technology. These covered improvements in all of the most important properties of a gamma-ray detector array namely: (i) high resolution providing extremely narrow full energy peaks, (ii) high efficiency for detecting incident gamma rays, (iii) high count rate capability, (iv) the collection of a high ratio of full-energy to partial-energy events, and (v) high granularity to reduce the probability of two gamma-ray hits in one

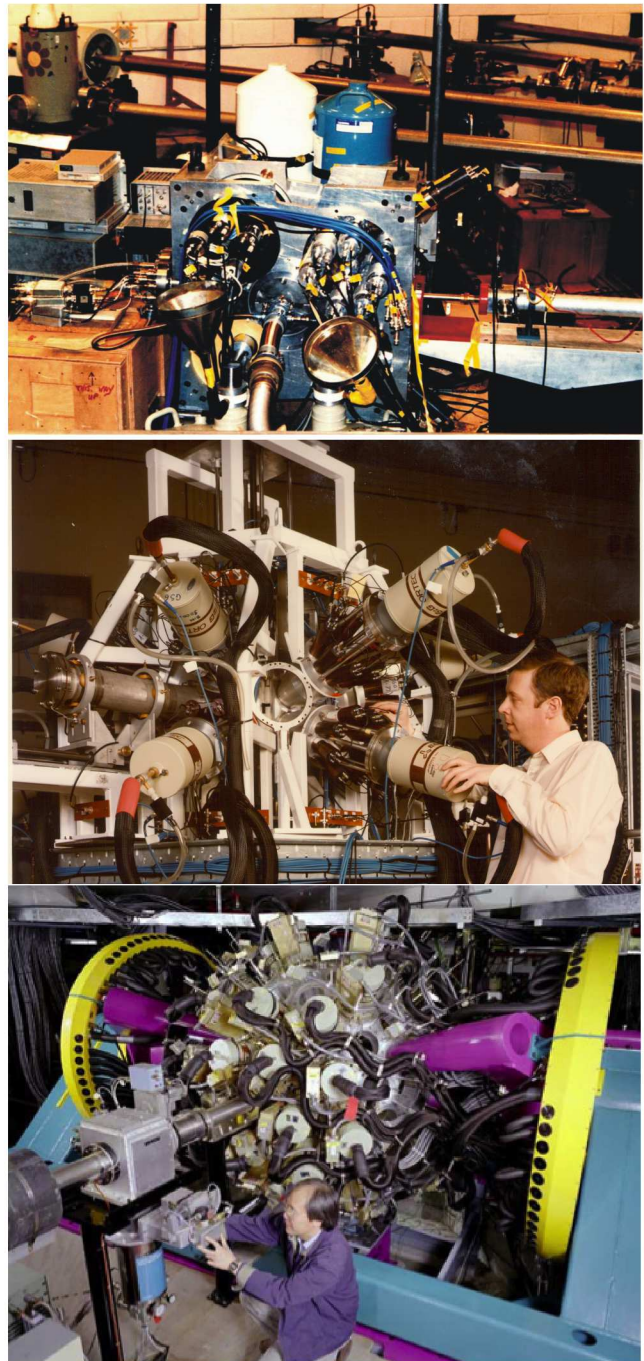


Fig. 6: The development of the escape-suppressed spectrometer arrays: From the original TESSA (5 ESS's) at NBI (top) to TESSA3 (16 ESS's) at Daresbury Laboratory (middle) to Gammasphere (110 ESS's) at LBNL and ANL (bottom).

detector from the same event and to localize individual gamma rays.

The size of Ge detectors themselves increased to improved overall efficiency and more escape suppressed spectrometers were assembled around a target, the latter being achieved by replacing NaI(Tl) by the more dense BGO in the suppression shield. Further increase in efficiency was obtained by assembling 4 or more Ge crystals in the same cryostat, for example to 4 crystal Clover detector [8], now

common in many arrays worldwide. In order to maintain and improve spectroscopic resolution the detectors were segmented on their outer contact to produce detectors with good position definition which enables better Doppler correction for in-beam experiments. Coupled with the detector developments were radical changes in the electronics and data acquisition systems. It was recognized that the signal outputs from the inner and outer contact were carriers of the knowledge of the interaction position in the crystal. This knowledge was extracted by digitisation of the output signals and using pulse shape analysis algorithms to extract the interaction position. Accurate time stamping of the pulse shapes to 10 ns accuracy was part of this technological revolution, enabling temporal as well as energy and position reconstruction of the events.

This is a time of great opportunity in nuclear spectroscopy and further technical advances are being made. This is being driven by the development of radioactive beam capabilities around the world which is opening a new landscape for discovery, and the connections between new nuclear structure studies and astrophysics, neutrino physics, and physics beyond the standard model are stronger than ever. First discussed in the early-1990's, the new technology of gamma-ray tracking, is poised to revolutionise gamma-ray spectroscopy in a similar way to how escape-suppressed detector arrays had done previously. Tracking arrays covering roughly 1π have been constructed in the US (GRETINA) and Europe (AGATA), see Fig. 7. Physics campaigns using both these devices have already begun. The momentum in developing this technology to its full potential will hopefully continue towards full 4π AGATA and GRETA spectrometers. The latter calorimeters will have unsurpassed sensitivity and discovery potential. These next generation arrays will be needed to greatly increase the reach of stable beam facilities as well as fully exploit the science opportunities at radioactive beam facilities. In addition, a wide range of important societal applications will benefit from gamma-ray tracking technology, such as PET and SPECT medical imaging systems, environmental monitoring, and many situations related to homeland security.

Moving towards a 4π Ge ball utilising the technique of gamma-ray energy tracking in electrically segmented Ge crystals is therefore the next major step in gamma-ray spectroscopy. The new tracking technique, as illustrated in Fig. 8, allows the identification of the energy and position of gamma-ray interaction points in the detector segments. Most gamma rays interact more than once within the crystal, and thus the energy-angle relationship of the Compton scattering formula is used to track the path of a particular gamma ray. Summing only the interactions belonging to a given gamma ray allows the full gamma-ray energy to be obtained. Thus scattered gamma rays between crystals are recovered and there are no vetoed Compton scatters in the suppression shields. The 4π gamma-ray energy tracking arrays, AGATA and GRETA, will have a high overall efficiency of $\sim 60\%$ for a single 1 MeV gamma ray. Other significant benefits include good peak-to-total ratio ($\sim 85\%$), high count rate (~ 50 kHz) capability per crystal, outstanding position resolution (~ 2 mm), the ability to record high multiplicity events without summing, the capability to select low-multiplicity events

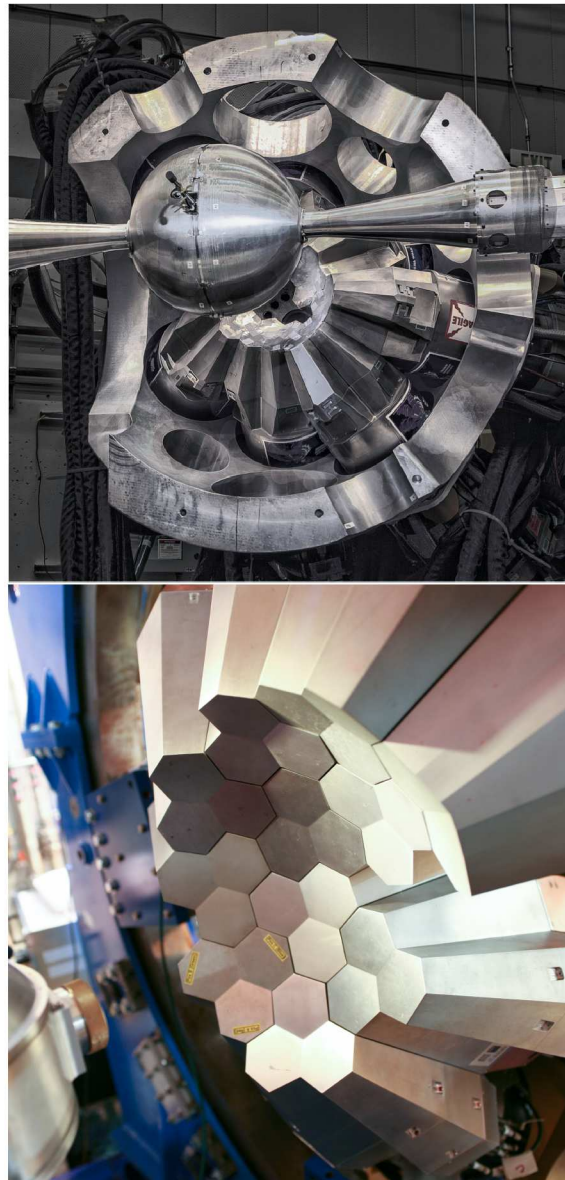


Fig. 7: The new generation of gamma-ray energy tracking arrays (top) GRETINA and (bottom) AGATA (courtesy of Patrice Lecomte - GANIL). These 1π systems will be fully developed into 4π arrays during the next decade.

hidden in a high back-ground environment, plus excellent linear polarization sensitivity. These 4π tracking arrays will provide orders of magnitude improvement in resolving power for many experiments as indicated in Fig. 2.

2. The Fascinating Angular Momentum Realm of the Nucleus

Nuclei at high angular momentum may be produced when an accelerated projectile nucleus collides and fuses with a target nucleus. The compound system first cools by evaporation of neutrons, protons and/or alpha particles. It then loses the rest of its excitation energy and almost all of its initial angular momentum by the emission of gamma rays. The total decay process is completed very quickly, in about 10^{-9} seconds. This process is illustrated in Fig. 9.

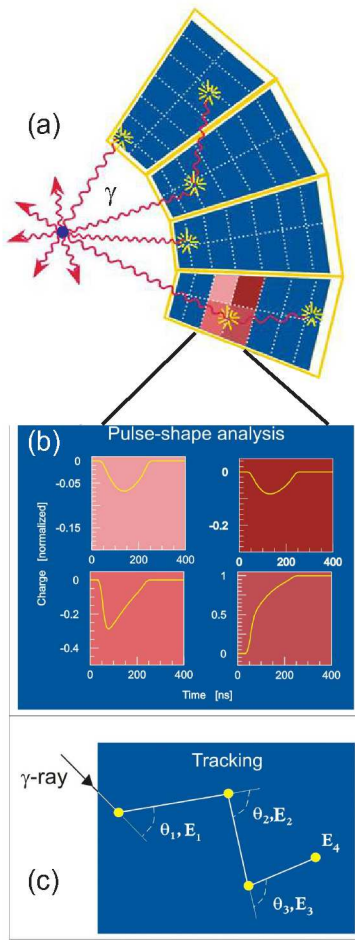


Fig. 8: Gamma-ray tracking technique principles. (a) Tracking arrays will consist of a closed shell of segmented Ge detectors. (b) Analysis of the pulse-shapes of signals from segments containing the interaction(s), transient signals in adjacent segments will also be analysed, thus allowing the measurement of the three-dimensional locations of the interactions, and their energies. (c) Tracking algorithms, based on the physics of the underlying physical processes such as pair production and Compton scattering, are used to determine the scattering sequence and identify the separate interactions of the gamma rays.

2.1. Creating nuclei at high angular momentum and high excitation energy

Atomic nuclei with their typical dimensions of several femtometers and rotation periods ranging from 10^{-20} to 10^{-21} seconds, are among the giddiest systems in nature. What makes the nuclear rotation very special and uniquely interesting are quantal effects due to the nuclear shell structure and superfluidity. Nuclei respond to the rotation in a rich and varied way. The crucial nuclear structure information is contained in the complicated details of the gamma-ray de-excitation flash when 30 or more gamma rays can be emitted. It is the detector system's job to cleanly catch as many of these gamma rays as possible. One of the greatest assets of modern detector arrays has been their ability to be used in conjunction with a wide range of auxiliary detector devices. These systems may detect protons, neu-

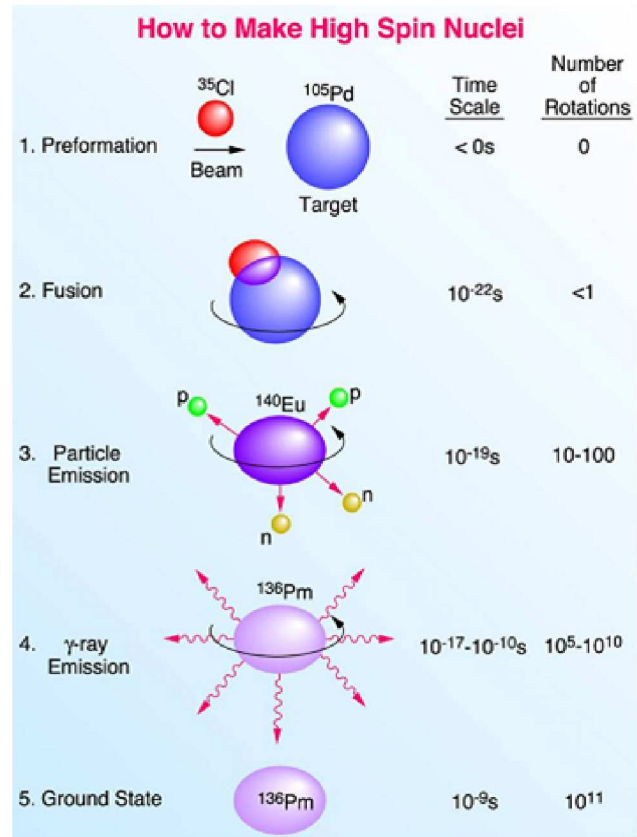


Fig. 9: How to create highly excited rapidly rotating nuclei.

trons, alphas and heavier particles involved in the reaction process in coincidence with gamma rays which enable new levels of sensitivity to be reached and also enormously increase the range of physics phenomena available for investigation.

A number of preferred pathways in the de-excitation process occur. They relate to favourable arrangements of protons and neutrons and can often be associated with specific symmetries or nuclear shapes. If a sufficient fraction of the decay flows down a particular quantized pathway or band, then the associated structure becomes observable and can be studied in detail.

2.2. Exotic nuclear structure phenomena in rapidly rotating nuclei.

The nucleus is a unique strongly interacting many-body quantal system that continues to reveal new phenomena (many of which are discussed in great detail within the present volume). Those related to high angular momentum structures, are represented schematically in Fig. 10. This list is by no means exhaustive, other important topics for example, include, chiral bands and wobbling excitations both associated with stable triaxial shapes. In Fig. 10 note that no states exist below the yrast line. For a comprehensive theoretical review of high-spin states in nuclei (in addition to the textbooks and references in the present article and special volume) which includes detailed discussion of many of these topics see Ref. [38] and references therein. Some of the observed phenomenon are:

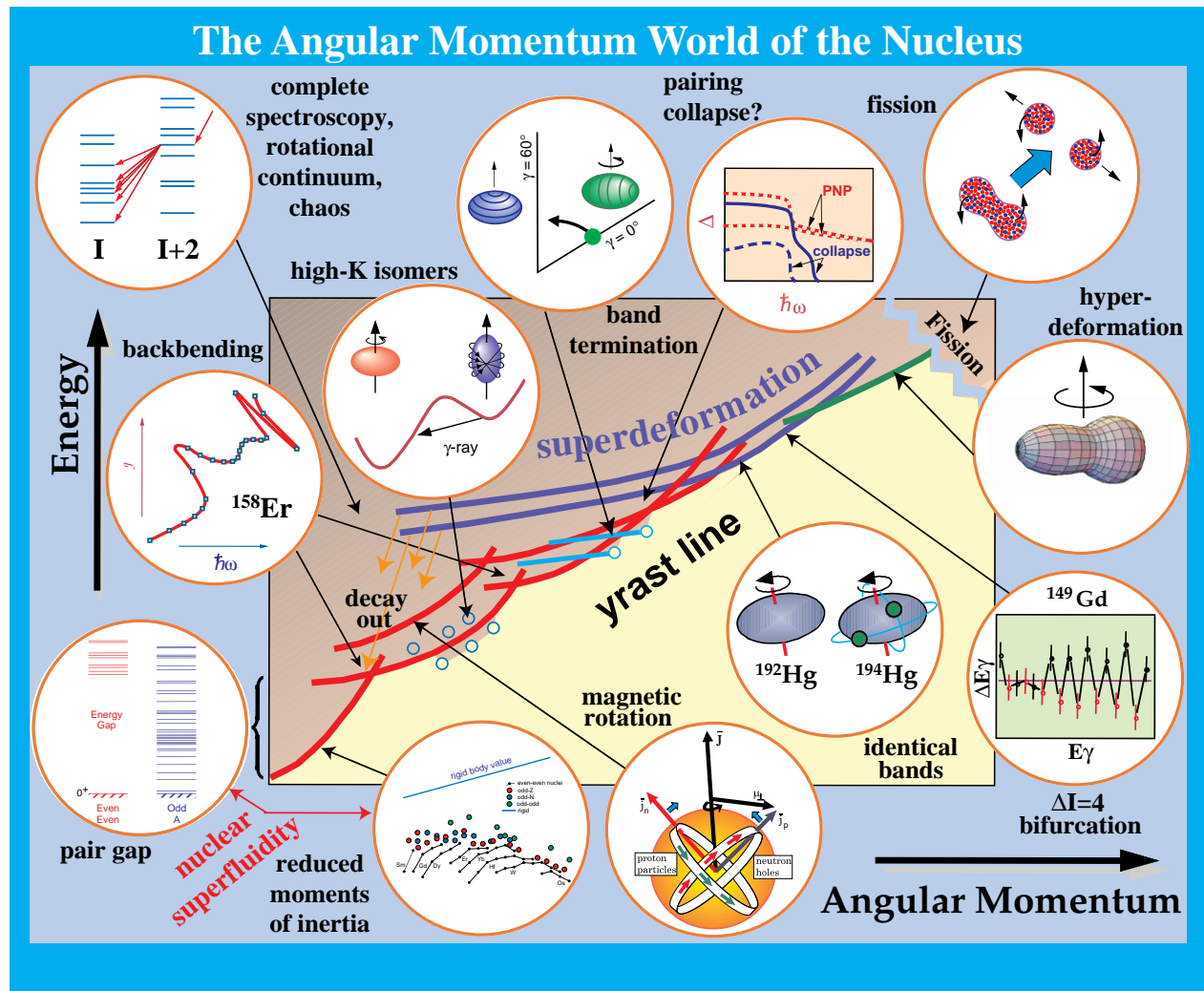


Fig. 10: Selected nuclear structure phenomena in rapidly rotating nuclei [28]. (Adapted by one of the authors from an original drawing by Witold Nazarewicz.)

• **Superdeformation** occurs when quantum shell effects help stabilize a rugby football shape (2:1 axis ratio in certain nuclei). Several regions of nuclei which possess this exotic second minimum in their potential energy landscape have been discovered. Superdeformed nuclei, now observed with axial and triaxial shapes, have been found to display some remarkable properties.

• **Identical Bands** are sequences of 10 or more identical photon energies associated with different bands in neighbouring nuclei. This came as a great surprise since it has long been believed that the gamma-ray emission spectrum for a specific nucleus represents a unique fingerprint. A consistent theoretical explanation of these patterns in a wide variety of nuclei is still lacking.

• **$\Delta I = 4$ Bifurcation** is the observation of extremely tiny (a fraction of a keV!) but very regular fluctuations in the energies of photons emitted from some superdeformed nuclei. They have been discussed by some theorists in terms of a tunneling motion at high angular momentum, but a complete explanation still remains elusive.

• **Band Termination** is the result of a gradual angular momentum induced shape transition from the deformed state of collective rotation to a non-collective configura-

tion, quantum mechanically forbidden to rotate. Such a “demise of the rotational band” which reveals the finite particle basis of the nuclear multi-fermion system, has been seen in a number of nuclei.

• **Reduction of Pairing Correlations with Rotation** is the quenching or total collapse of nuclear superfluidity at high rotational frequencies. The angular momentum behaves like an external magnetic field: it tries to align individual particle angular momenta along the axis of rotation, and this destroys correlations between nucleonic Cooper pairs.

• **Magnetic Rotation** is a new form of quantal rotor which occurs in nearly spherical nuclei and is characterized by sequences of gamma rays reminiscent of collective rotational bands but with a quite different character: namely, each photon carries off only one (rather than two) units of angular momentum and couples to the magnetic rather than electric properties of the nucleons.

• **Symmetry Scars** represent order in chaos. These are highly excited states that can be well described by quantum numbers in spite of a very large level density. Examples of such states are superdeformed bands or high-K isomers.

• **Hyperdeformation** has been predicted by many different calculations. It has been observed at low spins in the fission isomers in the actinide region [29, 30]. However at the dizziest nuclear states, extremely elongated nuclear shapes with the axis ratio of 3:1 or more are also expected to occur. Can these states survive in the presence of very strong centrifugal forces trying to split a nucleus apart? Many attempts have been made to produce and observe these states but so far none have been successful.

• **Above the yrast line moving up in energy and temperature**, new classes of phenomena may be explored. Examples include, the quasi-continuum and rotational damping, shape and pairing phase transitions, the goal of complete spectroscopy, giant resonances, the melting of shell structure and the transition from order to chaos.

3. The Discovery of High-Spin Nuclear Superdeformation and Identical Bands at Daresbury Laboratory

In 1984 the first sign of extremely elongated or “superdeformed” nuclear shapes at very high angular momentum or spin was observed at Daresbury Laboratory, see Fig. 11. Then a year later signals corresponding to superdeformed discrete states in ^{132}Ce and ^{152}Dy were discovered as previously shown in Fig. 5. These spectacular observations created a frenzy of activity into these exotic states both on the experimental and theoretical fronts. Such rapidly rotating nuclei were found to possess some remarkable properties. A number of major islands of nuclei where this phenomenon occurs were quickly discovered and explored within the next few years with many more seminal contributions coming from Daresbury Laboratory.

As mentioned previously nuclei are now known to display various shapes, for example, spherical, prolate (football shape), oblate (discus or doorknob shape), octupole (pear shape), triaxial etc. It is found that the short range attractive interaction among the constituent nucleons (protons and neutrons) is sufficiently strong to allow a small number of valence nucleons moving in anisotropic orbits to polarize and deform the whole nucleus. This means that neighbouring nuclei may exhibit quite different shape behaviour and indeed that different excitations within a single nucleus may lead to various shapes. Large regions of weakly deformed nuclei, ellipsoids with major to minor axis ratios of 1.3 to 1 are known to exist throughout the chart of nuclides. One of the most significant discoveries in nuclear structure physics of the last 40 years has been the observation of “superdeformed” nuclear shapes with major to minor axis ratios of around 2:1 at very high spin.

One successful theoretical approach has been to view the final shape of a nucleus as being governed by the interplay of two major contributions; a macroscopic (liquid drop) component describing the bulk properties of the nucleus and a microscopic (shell correction) component reflecting the quantal character of the orbitals occupied by the valence nucleons. The liquid drop concept works because the nucleons tend to interact only with their nearest neighbours rather like molecules in a liquid drop. Fig. 12 shows the single particle energy level spectrum of the sim-

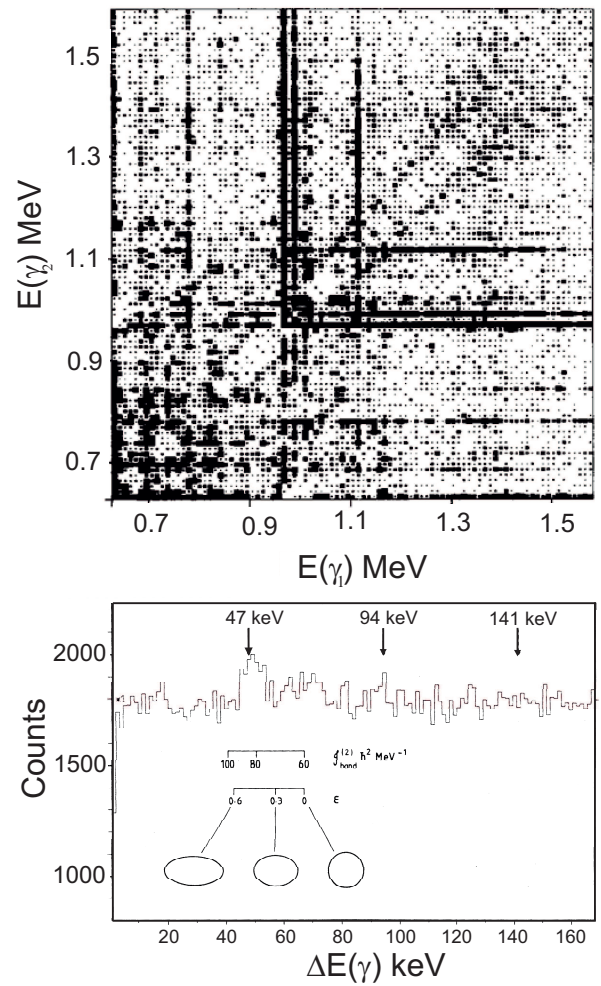


Fig. 11: (Top) The first observation of high-spin superdeformation in ^{152}Dy (using TESSA2) with ridges parallel and close to the $E(\gamma_1) = E(\gamma_2)$ diagonal in a 2D gamma-ray correlation spectrum. (Bottom) a projection of the ridges in the 2D matrix to highlight the ridges associated with a spacing of 47 keV. See Nyako et al., for details of this analysis [39]. Two years later an experiment using the same beam and target but now with TESSA3 revealed the main discrete band [32] associated with the ridge structure as shown in Fig. 5. Further experiments both at Daresbury Laboratory and elsewhere have revealed a rich spectroscopic world in the superdeformed minimum of ^{152}Dy , see Refs. [34, 40, 41, 42, 43] and references therein.

ple axially symmetric harmonic oscillator as a function of deformation. The large shell gaps at the particle numbers 2, 8, 20 etc. are responsible for these spherical nuclei, often referred to as “magic”, eg. ^4He , ^{16}O , ^{40}Ca etc being especially stable. This is analogous to the atomic shell closures in the noble gases. It is interesting to see that large shell gaps away from sphericity, corresponding to deformed magic numbers, are also present in Fig. 12 for deformations corresponding to when the lengths of the principal axes form integer ratios, e.g. 2:1, 3:1. (In more realistic potentials, with spin orbit effects included, this pattern is diluted but a fairly regular scheme of gaps still persists.) It is these quantal shell corrections which can be

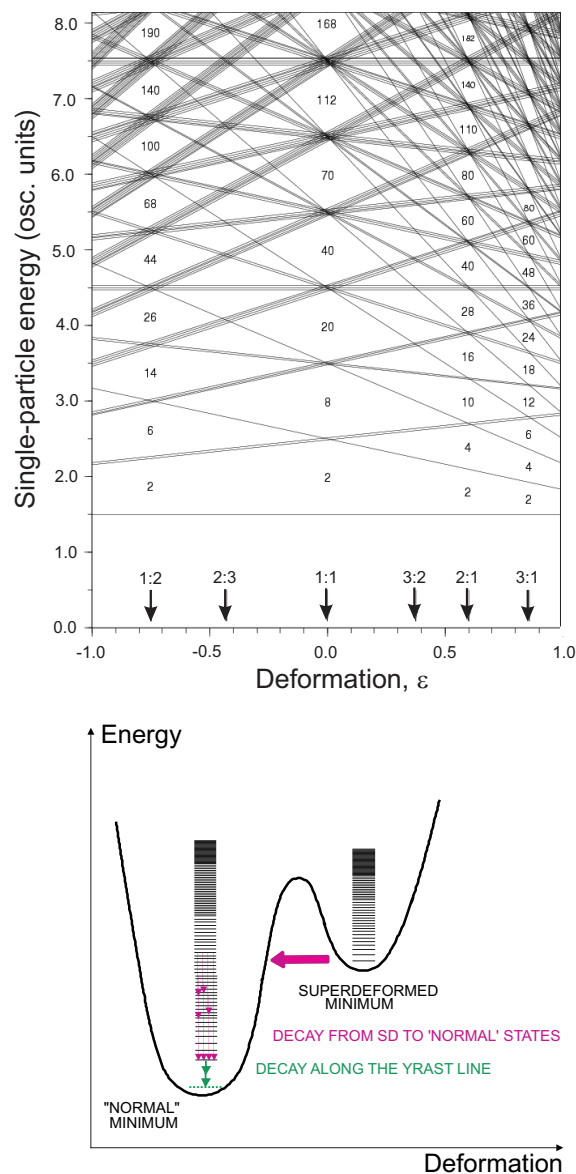


Fig. 12: (Top) Single-particle energy levels of the axially symmetric harmonic oscillator potential as a function of deformation parameter ϵ . The large shell gaps and corresponding magic numbers are indicated for spherical (1:1), superdeformed prolate (2:1) and superdeformed oblate (1:2) shapes. (Bottom) Two minima corresponding to normal deformed and superdeformed states.

sufficient when added to the liquid drop contribution under certain circumstances to lead to the stabilisation of a highly deformed nuclear shape, corresponding to a second minimum in the potential energy landscape [35, 36].

In the 1960's physicists studying the spontaneous fission of the heaviest ($A \sim 240$) nuclei discovered some unexpected properties which could only be explained if such a highly deformed second minimum existed in these nuclei. The presence of this deformed minimum was aided by the strong Coulomb repulsion present in these heavy nuclei balancing the surface energy which favoured more spherical shapes. These nuclei are known as the fission

isomers [37] and thus correspond to superdeformed nuclei. However their spectroscopic study is extremely difficult and restricted to very low spins.

In the mid 1970's it was realized by theoretical groups from Copenhagen, Dubna, Lund and Warsaw that not only did favoured shell corrections occur at 2:1 prolate shape for lighter nuclei (e.g. around $A=150$) but that in these cases this exotic shape can be stabilized and lowered in energy by the effects of rotational Coriolis and centrifugal forces. These calculations indicated that pronounced highly deformed minima occurred when favourable proton and neutron shell corrections coincided, leading to the prediction at high angular momentum of "islands of superdeformation" in the periodic chart.

As discussed in Section 2.1, nuclei at high spin or angular momentum may be produced using heavy-ion fusion evaporation reactions. The projectile and target fuse to form a compound nucleus at high excitation (e.g. 70-90 MeV) with angular momentum values up to the limit set by fission instability (e.g. $70\hbar$).

The gamma-ray signals from superdeformed states have very low intensity and it was not until the advent of multi-detector escape-suppressed γ -ray arrays in the 1980's that the first positive results were reported. The major breakthrough came in 1985 and 1986, at Daresbury Laboratory, England, when remarkable rotational spectra dominated by a long sequence (or band) of transitions was observed in ^{132}Ce and ^{152}Dy respectively, see Fig. 5. From the energy separation between transitions it was possible to determine the nuclear moment of inertia of these sequences. For ^{152}Dy this was consistent with that expected for a superdeformed 2:1 shape and a slightly less deformed shape for the rotational structure in ^{132}Ce . Conclusive evidence was obtained later when the intrinsic quadrupole moments of the bands were measured [40, 44].

These first results possessed some startling features, for example, (i) the energy spacing between transitions is remarkably constant, a feature which has led some physicists to refer to these objects as "nuclear pulsars" (ii) no link between the superdeformed states and the low spin normal deformed levels could be identified (iii) there is a sudden and dramatic depopulation of intensity at the bottom of the band over only one or two transitions.

Rapid progress was made following these initial discoveries at a large number of laboratories around the world and superdeformed bands were quickly observed in many other nuclei around ^{132}Ce and ^{152}Dy . Then soon after, in 1989, a new region of superdeformation was discovered at Argonne National Laboratory around $A \sim 190$ [45]. A number of significant discoveries, e.g. in $^{193,194}\text{Hg}$ [46, 47], also took place soon after at Daresbury Laboratory in this latter region. For more details on this extraordinarily productive period, along with a full set of historical references, see Refs. [48, 49, 50, 51]. In addition, for a most useful compendium of the numerous superdeformed bands and regions observed see Ref. [52]. No evidence for superdeformed oblate shapes has so far been observed, see Fig. 12.

From the observed gamma-ray energies we can extract important information on the moment of inertia behaviour as a function of spin or rotational frequency. Thus we can learn how the superdeformed nucleus responds to the stresses of rapid rotation. For example, as the number

of superdeformed bands observed in the $A=150$ region increased a pattern began to emerge. It was realized that the moment of inertia curve for a particular nucleus contained a fingerprint of the configuration or number of “intruder” orbitals that the valence particles occupied. These special orbitals originate from high- N oscillator shells and approach the Fermi surface at large deformations. This effect can be seen in Fig. 12. Because of their high intrinsic angular momentum these orbitals are strongly affected by the Coriolis force. Thus superdeformed spectroscopy offers the opportunity of giving us information about the behaviour and placement of such exotic orbitals that may not normally be accessible otherwise. In addition, from the moment of inertia behaviour we are also learning about the properties and stability of pairing or superfluid correlations in rotating highly elongated nuclear systems.

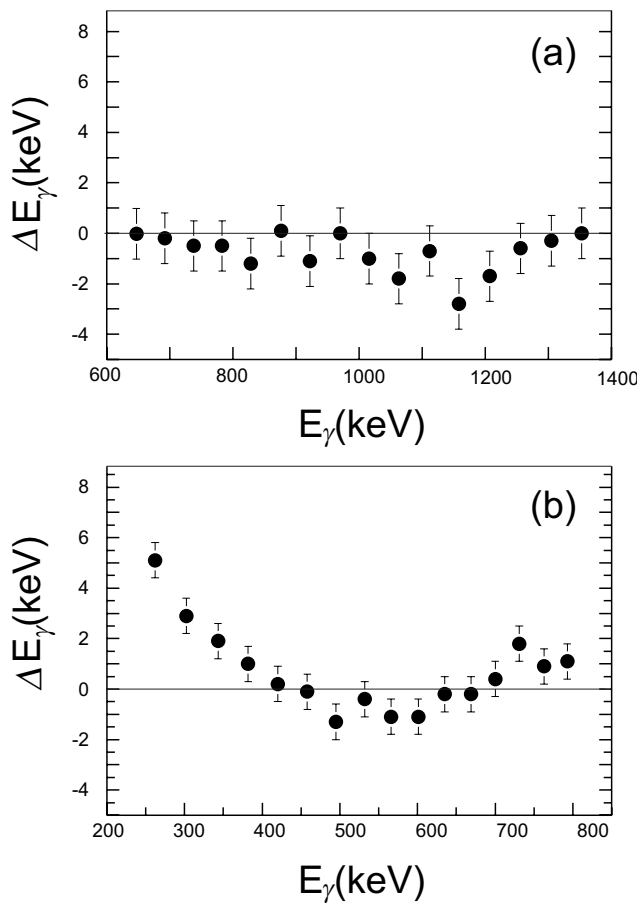


Fig. 13

The difference in gamma-ray energy between transitions in (a) the excited superdeformed band in ^{151}Tb and those in the yrast superdeformed band in ^{152}Dy and (b) the yrast superdeformed band in ^{192}Hg and an excited superdeformed band in ^{194}Hg , as a function of gamma-ray energy.

A major step forward in superdeformed spectroscopy occurred in 1989, again at Daresbury Laboratory, when excited or non-yrast bands were observed in a single nucleus. Such bands are particularly difficult to see since they are usually a factor of 2 or more weaker than the yrast superdeformed band. It was found that the moment of inertia of the excited band in ^{151}Tb , one proton less

than ^{152}Dy , followed extremely closely that of ^{152}Dy . This would imply the same high- N occupations for these two bands which can be understood in terms of particle-hole excitations. This is not so surprising. What was surprising and indeed unprecedented in nuclear physics was the fact that the γ -ray transition energies of these two bands were identical to within a few parts in 1000 over such a large spin and energy range [53, 54]! This is illustrated in Fig. 13.

These results were announced at a workshop in 1989 held at the Niels Bohr Institute where the identical or “isospectral” superdeformed bands in the ^{152}Dy - ^{151}Tb - ^{150}Gd cases were shown by Peter Twin to an amazed audience including Ben and Aage. At the same meeting it was also realized that the superdeformed band in ^{192}Hg was identical to an excited band in ^{194}Hg discovered at Daresbury Laboratory [46], and also shown for the first time at this historic meeting in Copenhagen, but only at high frequency [55, 56, 57], see Fig. 13. These results indicate that under certain circumstances, a superdeformed nucleus can be completely unaffected with the removal or addition of one or two nucleons. This is very surprising since there are a number of factors such as mass, deformation, pairing, orbital alignments etc which can, and usually do in normal deformed nuclei, alter the moment of inertia of neighbouring systems and hence their relative transition energies by tens of keV. Other examples soon followed in the $A=150$ and 190 regions. The latter region in fact has turned out perhaps to be the most prolific in this phenomenon and with some important additional features. For example, data from Daresbury Laboratory in ^{193}Hg constituted the first conclusive experimental evidence for identical superdeformed bands in the same nucleus [58].

It seems that some subtle cancellations are taking place or more interestingly that these degeneracies are the result of some underlying symmetry not yet recognized! Many speculations have been made involving symmetries and modes of excitation not previously observed in nuclei. In addition evidence for identical bands in normal deformed nuclei was searched for and found. Comprehensive reviews of identical bands in superdeformed and normal deformed nuclei can be found in Ref. [59, 60].

But before leaving this topic we must mention the even more puzzling phenomenon of $\Delta I = 4$ bifurcation in identical superdeformed bands discovered by the Chalk River Group. It was observed that states differing by four units of spin showed a consistent energy shift of about 60 eV indicating the presence of a new quantum number associated with a fourfold rotational symmetry. Since this remarkable discovery was not found at Daresbury Laboratory we will not discuss it further here but instead refer the reader to Refs. [61, 62, 63] as well as the article by Ward, Waddington and Svenssen to this volume [64].

4. The Spectroscopy of ^{158}Er through the Decades

In the realm of high spin nuclear physics, the rare earth region has been one of the most popular for experimental studies since nuclei here can accommodate the highest values of angular momentum. In particular, in the nucleus ^{158}Er numerous fascinating phenomena have been observed with increasing angular momentum and excita-

tion energy as shown in Fig. 2. This special nucleus has often been used as a textbook example of the evolution of nuclear structure [65, 66, 67, 68, 69, 70, 71, 72, 73] and is discussed further below. In addition, ^{158}Er , because of its interesting shape coexistence features at high angular momentum, was used as the test case example for the development of the Ultimate Cranker Code [74].



Fig. 14: An short movie about backbending or rotational alignment in nuclei [75] can be downloaded and viewed at <http://www.physics.fsu.edu/TheBackBender> [76]. It contains a mechanical analog utilizing rare-earth magnets and rotating gyroscopes on a turntable along with some historic spectra and papers associated with the discovery of this game changing phenomenon. Backbending was a major surprise which pushed the field forward but it is now sufficiently well understood that it can be used as a spectroscopic tool providing useful insight for example, into nuclear pairing correlations and changes due to blocking effects and seniority, nuclear deformation, the configuration of rotational structures and the placement of intruder orbitals at the Fermi surface. See, for example, the articles discussing the history of backbending in nuclei in Ref. [77] along with the textbooks referenced in the present article.

4.1. Level structures up to band termination in ^{158}Er

In ^{158}Er , as the angular momentum increases, this nucleus exhibits Coriolis-induced rotational alignments [75] of both neutron and proton pairs along the yrast line, see Figs. 2 and 10. It was among the first in which backbending, i.e., rotational alignment of a pair of high- j neutrons (see Figs. 10,14,15), was discovered (spin $I \sim 14$) [78],

and it was the first nucleus where a second alignment, of high- j protons, at $I \sim 28$ [79] and a third anomaly at $I \sim 38$ [80] in the moment of inertia along the yrast line were identified. When spin values reach 40 - 50 (see Refs. [81, 82, 83]), a very different structure becomes most energetically favoured (i.e. yrast), where this nucleus undergoes a dramatic shape transition from a collective prolate (rugby or American football shape) rotation to non-collective oblate (flattened sphere shape) configurations. The latter terminates at an energetically favoured state where all the valence nucleons outside the Gadolinium-146 (^{146}Gd : $Z = 64$, $N = 82$) semi-magic spherical core have their spins fully aligned in the same direction, see Figs. 16,17.

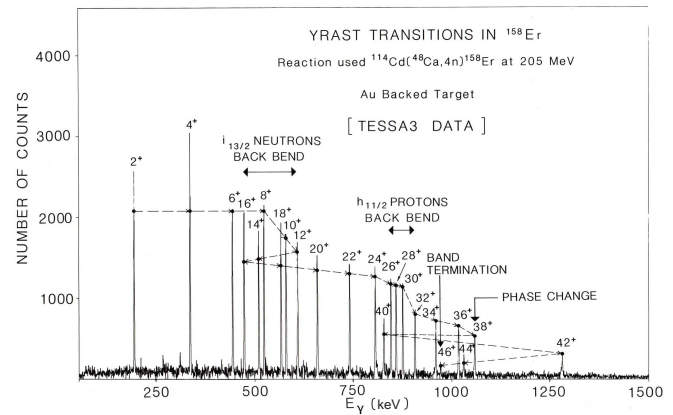


Fig. 15: The yrast band in ^{158}Er up to the favoured band termination state at $I^\pi = 46^+$ obtained using the TESSA3 spectrometer. This spectrum has been used in a number of textbooks.

Band termination represents a clear manifestation of mesoscopic physics, since the underlying finite-particle basis of the nuclear angular momentum generation is revealed. In ^{158}Er , three terminating states, $I^\pi = 46^+$, 48^- , and 49^- , have been observed, see Figs. 2, 17. Other neighbouring nuclei were also found to exhibit similar fully aligned states which provided stringent tests of nuclear models since the wavefunctions for these special states are extremely pure.

4.2. Level structures beyond band termination in ^{158}Er

Establishing the nature of the states in the rare earth nuclei well beyond the very favoured band terminating states had been a goal for several decades. Several years ago, a number of weak, individual transitions feeding into the terminating states were observed in ^{158}Er (and its neighbour ^{157}Er [86, 87]), but this only extended the highest spin by 1 - $2\hbar$. The related levels above band termination have been suggested to arise from weakly collective single-particle excitations that break the ^{146}Gd core. More significantly, in 2007, rotational structures, displaying high dynamic moments of inertia and possessing very low intensities ($\sim 10^{-4}$ of the respective channel intensity), in ^{158}Er

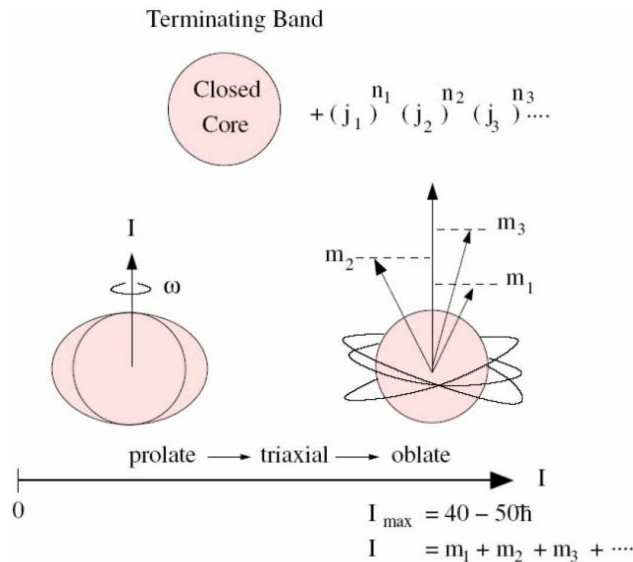


Fig. 16: Schematic illustration of a band terminating configuration built from a closed core plus a number of nucleons in partly filled j-shells. In the lower part, the evolution with spin is illustrated, from prolate and collective rotation at low spins to an aligned oblate state at the termination. Adapted from [84].

(and ^{157}Er) were identified [88]; see Figs. 18, 19. These structures bypass the “band terminating” states and extend over a spin range of $\sim 25 - 65\hbar$, marking a spectacular return to collectivity at spins beyond band termination, see Fig. 2. These sequences have properties, for example, moment of inertia values that are very different from the lower spin states. Thus, a new frontier of discrete-line gamma-ray spectroscopy towards spin $\sim 70\hbar$, the so-called “ultrahigh-spin regime”, in ^{158}Er was opened.

The new ultrahigh spin bands in ^{158}Er (and ^{157}Er) were proposed to be triaxial strongly deformed (TSD) structures. This was consistent with the predictions of the early cranking calculations of Bengtsson and Ragnarsson [91] and Dudek and Nazarewicz [92].

In nuclear physics, stable asymmetric or triaxial shapes are a long-standing prediction of theory [1], and had been sought after for decades. However, it was not until 2001 that compelling evidence for nuclei with a robust triaxial shape was revealed in the rare-earth region in Lu nuclei ($Z = 71$ and $A \sim 165$) through the observation of rotational structures associated with the unique “wobbling” excitation mode [89, 93].

A triaxial nuclear shape has distinct short, intermediate, and long principal axes. This shape is commonly described using the parameters (ε_2, γ) of the Lund convention [94], where ε_2 and γ represent the eccentricity from sphericity and triaxiality, respectively. Collective rotation about the short axis, corresponding to a positive γ value ($0^\circ < \gamma < 60^\circ$), usually has the lowest excitation energy at high spin due to moment of inertia considerations [65, 95]. This mode is thus expected to be favoured over rotation about the intermediate axis ($-60^\circ < \gamma < 0^\circ$). In ^{158}Er , configurations with $\varepsilon_2 \sim 0.34$ and a positive value of $\gamma = 20^\circ - 25^\circ$ were theoretically predicted to be low in energy and, were thus initially suggested in the interpretation of

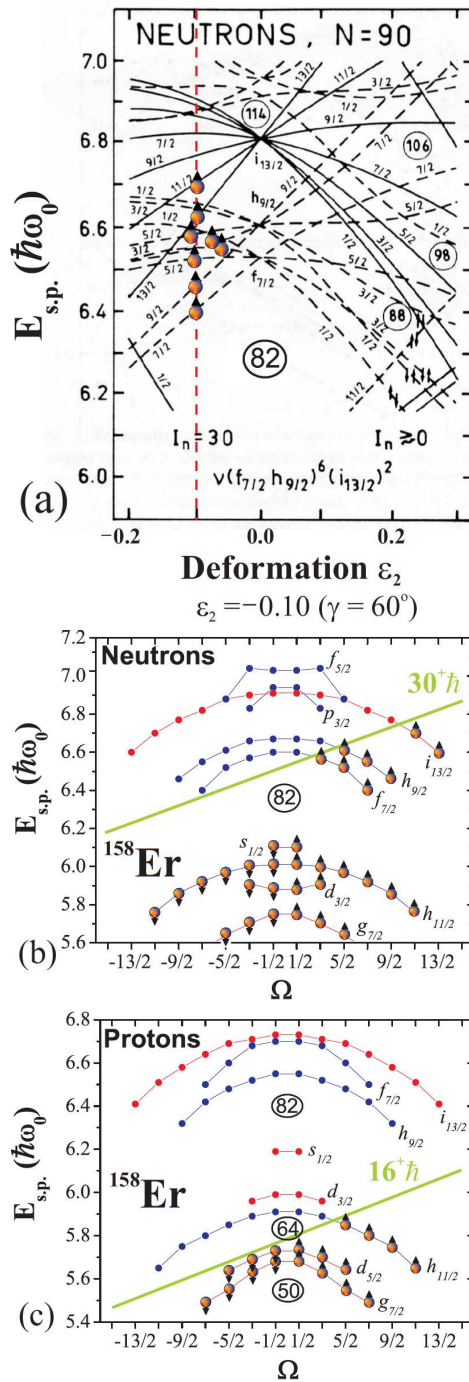


Fig. 17: (a) Nilsson diagram showing the 8 valence neutrons of ^{158}Er , outside the closed $N = 82$ shell, and the orbits they occupy at $\varepsilon_2 = -0.10$. (b) Tilted Fermi Surface plot ([65]) for neutrons, illustrating how the 8 valence particles, above $N = 82$, generate $I^\pi = 30^+\hbar$ based on which orbitals they occupy. (c) Tilted Fermi Surface plot for protons, illustrating how the 4 valence particles, above $Z = 64$, generate $I^\pi = 16^+\hbar$, based on which orbitals they occupy. The coupled proton and neutron configurations from (b) and (c) lead to the 46^+ terminating state in band 2 of ^{158}Er . In both (b) and (c), the core of $N = 82$ and $Z = 64$ does not contribute to spin. Note that to make the fully aligned 48^- and 49^- states (see Fig. 2) the least favoured $h_{9/2}$ and $f_{7/2}$ neutron respectively is promoted to the $\Omega = 9/2$ $i_{13/2}$ level. Adapted from [84, 85]

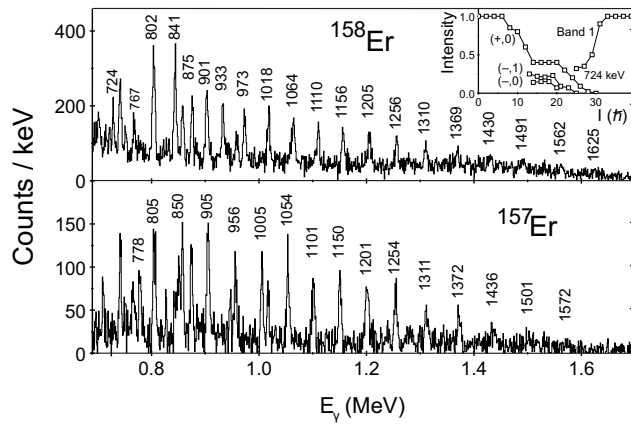


Fig. 18: Background-subtracted coincident γ^5 spectra illustrating the two strongest sequences observed in ^{158}Er (top) and ^{157}Er (bottom) [88]. The relative intensity profiles of the new (band 1) sequence in ^{158}Er and known structures around the feedout region are shown in the inset providing an indication of the associated spins for the band.

the collective bands at ultrahigh spin [88].

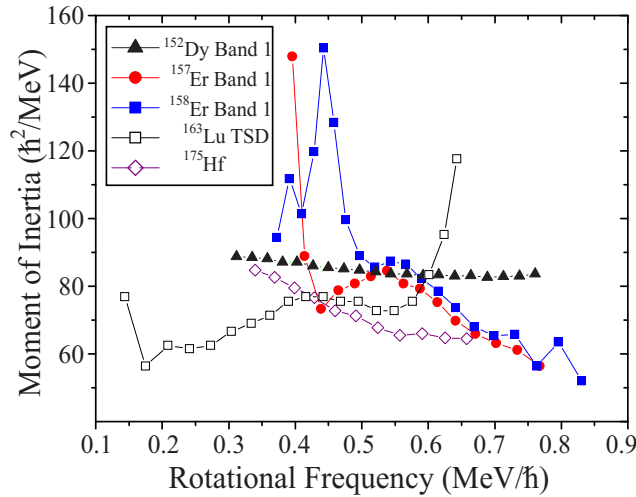


Fig. 19: Dynamic moments of inertia as a function of rotational frequency for the Band 1 sequences in $^{157,158}\text{Er}$ compared with other strongly or super deformed bands in the region, e.g., the yrast SD band in ^{152}Dy [32], a TSD band in ^{163}Lu [89], and ^{175}Hf [90]. Taken from Ref [88].

An experiment to measure the transition quadrupole moments of the observed ultrahigh spin sequences in $^{157,158}\text{Er}$ was carried out using the Doppler Shift Attenuation Method (DSAM) and the Gammasphere spectrometer. More details of this DSAM experiment can be found in Ref. [96]. Compared with the previous thin-target experiment [88], the improved statistics of the DSAM experiment made possible the observation of a third collective band at ultrahigh spin in ^{158}Er (band 3). This new sequence, band 3, had an intensity of $\sim 10\%$ of the strongest collective band (band 1). Despite their very low intensities, an analysis of fractional Doppler shifts $F(\tau)$ was possible for the three bands in ^{158}Er to determine their transition quadrupole moments Q_t [96, 97].

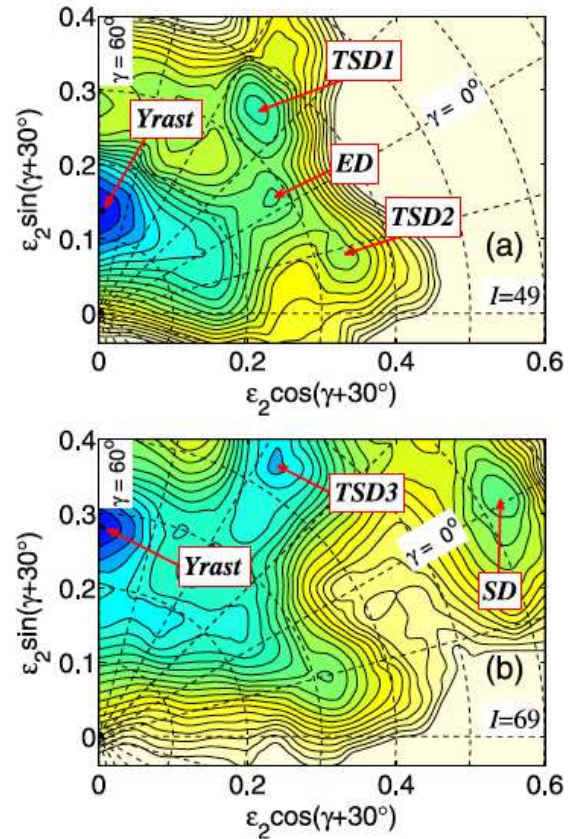


Fig. 20: Potential energy surfaces in ^{158}Er calculated for negative parity and signature $\alpha = 1$ at spins $I = 49$ (a) and 69 (b), respectively. The contour line separation is 0.25 MeV. The minima of interest are labelled (see text).

The Q_t of the three collective bands at ultrahigh spin in ^{158}Er have been determined to be $\sim 9-11$ eb demonstrating that they are all associated with strongly deformed shapes. By comparison, the low spin yrast band in ^{158}Er has a measured Q_t of ~ 6 eb [98]. The measured Q_t values however are larger than expected for the energetically favoured positive- γ (rotation about the short axis) triaxial shape (TSD1: $\epsilon_2 \sim 0.34$). Rather, they are more compatible with a negative- γ (rotation about the intermediate axis) triaxial deformed minimum (TSD2: $\epsilon_2 \sim 0.34$) or a positive- γ minimum with larger deformation (TSD3: $\epsilon_2 \sim 0.43$) within the current cranked Nilsson-Strutinsky (CNS) theoretical framework [99], see Fig. 20. Another “calibration” measurement on ^{154}Er was performed under very similar experimental conditions [100], where the Q_t of the yrast superdeformed band in ^{151}Dy was extracted. The measured value of this experiment agreed with the reported one of Ref. [101] and is reproduced well by the CNS calculations for a prolate superdeformed shape. It thus provided a consistency check for the experimental approach and the stopping powers, which are well known to cause a systematic uncertainty of $\sim 15\%$ in the Q_t value from a DSAM experiment.

This puzzle in the experimental quadrupole moment measurements triggered further theoretical studies. For example, calculations using the 2-dimensional tilted axis cranking (TAC) method [102] based on a self-consistent

Skyrme-Hartree-Fock (SHF) model were performed for ultrahigh spin configurations associated with triaxial shapes in ^{158}Er [103]. These calculations showed that the negative- γ minimum (rotation about the intermediate axis) is a saddle point and therefore the TSD2 minimum should not be considered as a physical candidate. The Q_t calculated for a positive- γ triaxial minimum configuration with large deformation (~ 10.5 eb), which is similar to the TSD3 minimum mentioned above, is consistent with the experimental values. Nevertheless, this minimum does not become yrast until spin $\sim 70\hbar$. However an open question remains as to “where are the band structures associated with the most energetically favoured TSD (TSD1) minimum”? Other recent theoretical investigations into the ultrahigh spin bands in ^{158}Er and neighbouring nuclei [104, 105, 106] have added to the ongoing story of ^{158}Er at ultrahigh spin. Indeed, in [106] it is stated that “If the theoretical spin assignments turned out to be correct, the experimental band 1 in ^{158}Er would be the highest spin structure ever observed. The current study stresses the need for more precise measurements of Q_t and reliable estimates of spins in these bands.”

Other questions arise from the above observations of collective sequences at spins beyond band termination in ^{158}Er . For example, are such structures a common feature of the light rare-earth nuclei and how do their properties change as a function of N and Z ? Since multiple bands are observed, for example, in $^{157,158}\text{Er}$, could some of these sequences be wobbling excitations at ultrahigh spin and if so how do they differ from wobbling bands in Lu nuclei at lower spins? In fact, the recent discoveries in ^{158}Er have triggered a comprehensive experimental project to investigate light rare earth nuclei ($A \sim 150 - 165$) to study this phenomenon. So far ultrahigh spin collective bands with similar characteristics to $^{157,158}\text{Er}$ have been observed in ^{154}Er [100, 107], $^{160,161}\text{Tm}$ [108] and $^{159,160}\text{Er}$ [109]. In the $N = 90$ isotones ultrahigh spin TSD candidate bands have also been observed in ^{160}Yb [110] and ^{157}Ho [97].

A primary nuclear structure goal is to bridge our understanding of the evolution between the high spin SD (superdeformed) regime of the Gd, Tb, and Dy nuclei (^{152}Dy [32], for example) and the lower spin TSD/Wobbling domain centered on Lu nuclei (^{163}Lu [89, 93], for example) and neighbouring nuclei such as ^{167}Ta [111]. A fully consistent picture as to the nature of the nucleus in the ultrahigh spin triaxial world thus remains to be uncovered. These results point to the need for further experimental investigations.

5. The Demise of Pairing Correlations at High Spin in $A \sim 160$ Er Nuclei

The evolution of the superfluid properties of the nucleus with increasing angular momentum has been [1] and continues to be of considerable interest. For an excellent summary of this particular topic and other aspects related to pairing correlations in nuclei, including backbending and quasi-particle alignments, the reader is referred to Ref. [77] “Fifty Years of Nuclear BCS: Pairing in Finite Systems”. At low spins, the nucleus displays well-established superfluid properties with nucleons pairing up in time-reversed orbits, or Cooper pairs. But collective rotation of the nu-

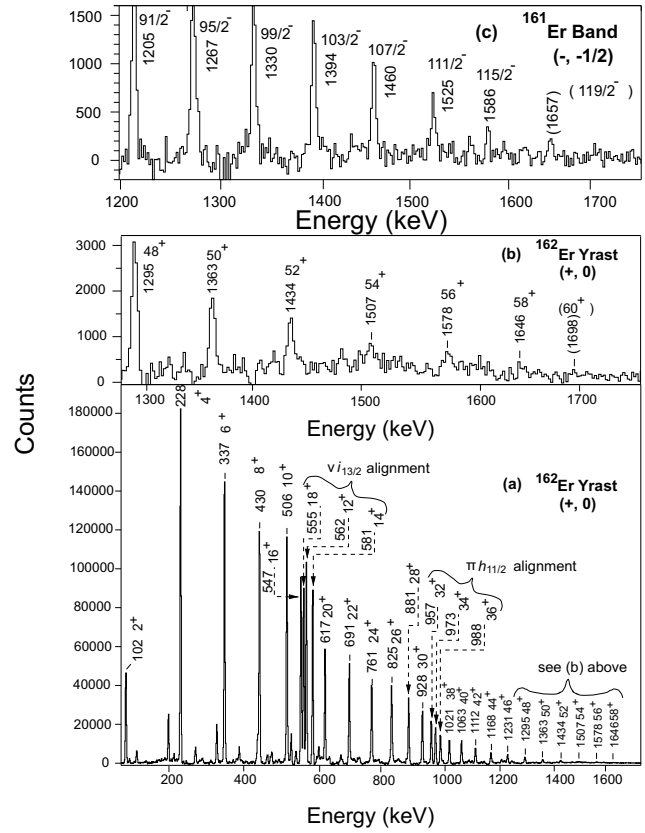


Fig. 21: Spectra showing the yrast band in ^{162}Er (a,b) along with the lowest energy negative parity band in ^{161}Er (c) up to spin values around $60\hbar$ [115].

cleus tries to break these correlated fermions apart, the Coriolis anti-pairing effect. With increasing rotational frequency and particle alignments it was thought that a transition out of the superfluid paired phase may occur, in an analogous manner to the quenching of superconductivity by a sufficiently high magnetic field (the Meissner effect). However, while it now seems that the occurrence of such a phase change is somewhat more complex in nuclei than at first thought, “the question of how does rotation affect the pairing correlations at very high spin is still an important and unfinished business” (Ben Mottelson, NBI 1997).

The observation of band crossings at high spin is one means of knowing if static pairing correlations exist. In addition if pairing is significant then allowed band crossing are expected at similar rotational frequencies. In the absence of pairing, a band based on a particular single-particle configuration can be crossed by another rotational band based on a different but more energetically favourable configuration. The rotational frequencies at which such rearrangements take place depend on the detailed single-particle spectrum of states. The observation of crossings at high angular momentum that are not correlated in rotational frequency would be a characteristic of the decline of static pairing correlations.

In a series of experiments, which began at Daresbury Laboratory on the TESSA 2 and 3 and Eurogam arrays, then Euroball at Legnaro National Laboratory in Italy and Gammasphere at Lawrence Berkeley National Laboratory in the USA, the transitional nuclei ^{159}Er - ^{162}Er [112, 113,

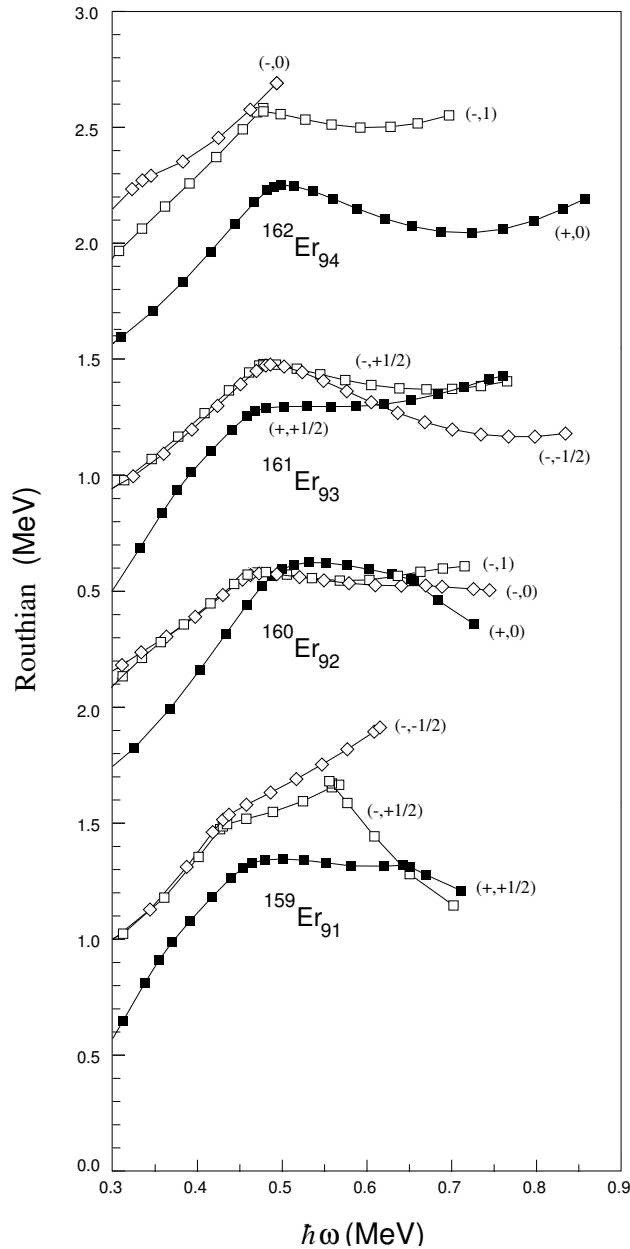


Fig. 22: Experimental Routhians for the high-spin sequences in $^{159,160,161,162}\text{Er}$. The data are taken from [115, 112]. A constant moment of inertia (J_0) of $72 \text{ MeV}^{-1}\hbar^2$ is used as a reference for these Routhians.

114, 115] have been observed to very high spin ($I=50-60\hbar$), see Fig.21.

The experimental Routhians for high rotational frequency are plotted in Fig.22 for the Er nuclei. A constant moment of inertia (J_0) of $72 \text{ MeV}^{-1}\hbar^2$ is used as a reference for these Routhians. In Ref.[112] the anomalous band crossing in the $(-, +\frac{1}{2})$ sequence near $\hbar\omega=0.55 \text{ MeV}$ ($\approx \frac{81}{2}$) in ^{159}Er could not be attributed to a regular quasiparticle alignment in a paired regime. This anomalous crossing and the energy ordering of the bands could however be explained in the unpaired regime in terms of the occupation of specific single-neutron orbitals.

The neutron orbital scheme was extended to the high spin states ($\sim 45-50\hbar$) in $^{161,162}\text{Er}$ observed in a subse-

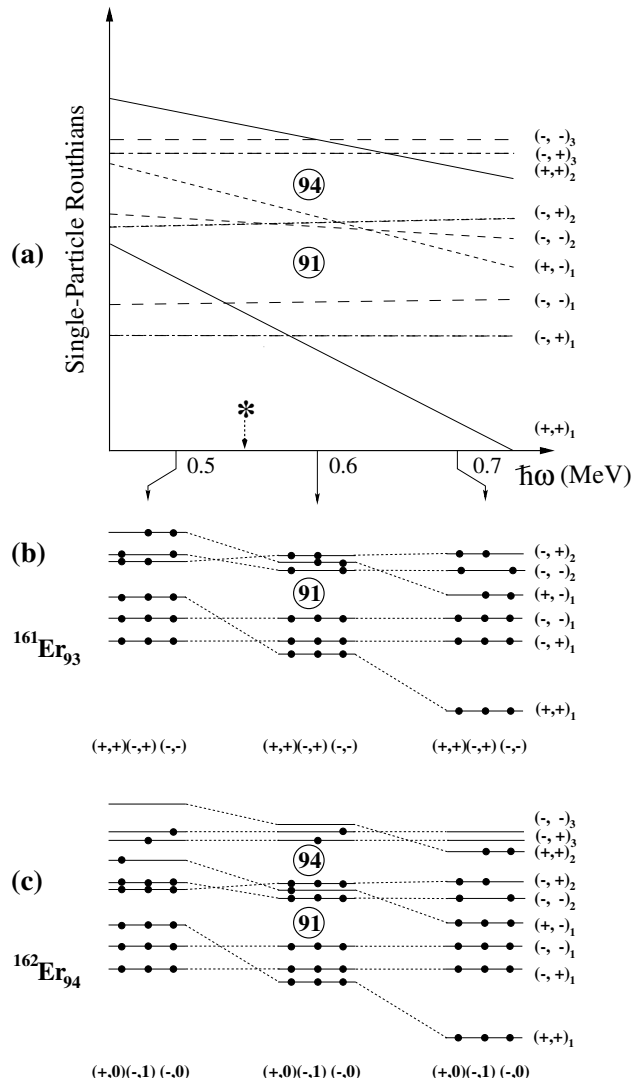


Fig. 23: (a) Schematic of single neutron energy levels expected without static pairing correlations. The * near a rotational frequency of $\hbar\omega = 0.55 \text{ MeV}$ indicates where the band crossing in the $(-, +\frac{1}{2})$ sequence in ^{159}Er occurs. The values for the frequency are indicative. (b) and (c) show the occupation for the three lowest energy (π , α) configurations in ^{161}Er and ^{162}Er at three rotational frequency values. The ' $\frac{1}{2}$ ' for the signature (α) labels has been omitted for clarity.

quent experiment where it once more was found to be surprisingly successful [113]. The schematic single-neutron Routhians used for $^{161,162}\text{Er}$ is shown in Fig.23 (a). The frequency scale is approximate but is in line with more realistic calculations based on the Nilsson model allows an approximate frequency scale to be added to figure 5(a). Fig. 23 (b) and (c) show the occupation for the three lowest energy (π , α) configurations in ^{161}Er and ^{162}Er , respectively, at three rotational frequency values. The model predicts that the $(-, -\frac{1}{2})$ band in ^{161}Er remains yrast at high spin and that the $(-, +\frac{1}{2})$ sequence will become lower in energy relative to the $(+, +\frac{1}{2})$ band above $\hbar\omega \geq 0.6 \text{ MeV}$. In these regards this model is consistent with the experimental results, see Fig.22. The model also predicts that the uppermost pairs of valence neutrons are

not rearranged, i.e the (π, α) remains unchanged, until extremely high frequency in ^{161}Er , $\hbar\omega \approx 0.9$ MeV, which is well above the highest frequency observed. For ^{162}Er the model is consistent with the observation of the $(+,0)$ band remaining yrast at high spin.

The consistency between this basic unpaired model and the data supports the suggested spectrum of single-neutron states at these particle numbers and deformation. However, this simple model does have its limitations, for example no deformation changes or consideration of different proton occupations are considered. Therefore, in order to investigate and interpret the detailed behaviour of the high spin structures further, cranked Nilsson–Strutinsky calculations, based on the configuration–dependent formalism, were performed to compare with experiment, see [115, 116]. In these calculations both neutron and proton pairing correlations are neglected and fixed configurations can be traced as a function of spin. Different bands are formed by searching for the lowest energy solutions within a particular configuration. The calculations predict that the high spin yrast states are dominated by a series of rotational bands which maintain their prolate shape ($\varepsilon_2 = 0.20\text{--}0.25$, $\gamma \approx 0^\circ$) up to $\approx 65\hbar$ in both ^{161}Er and ^{162}Er . There is good overall agreement between these calculations and the experimental results giving strong evidence for the demise of static pairing correlations at these very high spin values.

In summary, experiments with Euroball and Gammasphere have allowed detailed spectroscopy to be carried out in the spin 50 to 60 regime in a range of Er isotopes. This has enabled us to gain some insight into the behaviour of the atomic nucleus in the absence of static pairing correlations and to investigate shape competition at the very highest excitation energy and angular momentum. Further experiments in this area will be required since it is important to investigate band crossing frequencies in a range of nuclei. Indeed at the same time as discoveries were made in the Er isotopes, unpaired crossings were also being discovered in neighbouring nuclei, e.g ^{156}Dy [117].

6. The Termination of Rotational Bands: Abrupt and Smooth

Two types of band termination have been observed to occur in nuclei. The first involves the crossing, in terms of excitation energy, of deformed collective rotational states and oblate non-collective single-particle states, the latter becoming favoured at high-spins. This is often called “abrupt” band termination. The second type, which has been called “smooth” or “soft” band termination, results when, for a given configuration, a deformed collectively rotating nucleus gradually changes its shape over several units of spin from a prolate to a non-collective oblate shape. Detailed discussions of band termination can be found in the review article by Afanasjev et al. [118].

The transitional erbium isotopes exhibit perhaps the classic examples of the angular momentum induced abrupt prolate-collective to oblate non-collective shape change at high spin in heavy nuclei [84, 118], as discussed in Section 3.1. Some of the best examples of smoothly terminating bands have been found in the $A \sim 110$ mass region [118, 119, 120], see the article by Ward, Waddington and

Svensson [64] in the present volume for more information about the discovery of this phenomenon.

In the $A \sim 110$ nuclei the structures are based on configurations with a few valence nucleons outside the ^{100}Sn closed core. It would be interesting if a link between the smooth terminating bands in the mass 110 region were made to the superdeformed configurations in the mass 130 region by observation of the latter to terminate. Indeed, the existence of smoothly terminating structures in the superdeformed bands in $A \sim 130$ nuclei was predicted some time ago by Afanasjev and Ragnarsson using cranked Nilsson–Strutinsky calculations [121]. However, because the terminating spins were expected to be very high (e.g. ≥ 70 in ^{132}Ce) it was believed that it would be too difficult to observe such states. Subsequent studies have revealed the first hint for smooth band termination behaviour in the yrast superdeformed band in ^{132}Ce [122, 123] which was featured earlier in this article.

To push to even higher spins requires the power of the full tracking spectrometers AGATA and GRETA. It may be possible using one of these next generation spectrometers, together with a very high fold coincidence analysis, to get to these extreme spin values. An encouraging glimpse of such an analysis is shown in Fig. 24 from data taken using Gammasphere [123]. The spectrum displays the lowest energy superdeformed band in ^{132}Ce in coincidence with eight transitions. Amazingly, as the lower panel shows, the band even survives in an 11 fold spectrum.

7. Summary and Conclusions

High resolution gamma-ray spectroscopy has proven itself to be pivotal tool in the study of the structure of atomic nuclei. In recent decades many significant experimental advances have taken place. Fascinating and often surprising new aspects of nuclei at the limits of isospin, excitation energy, angular momentum, temperature, and mass continue to be revealed.

In this article we have focussed on high spin investigations that started at the Niels Bohr Institute in Denmark and Daresbury Laboratory in the UK in the late 1970’s and early 1980’s on several rare-earth nuclei and have continued, due to their compelling nature, through the decades to the present day. The exciting experimental quest to even higher spins ($\sim 60\text{--}80$) will continue in these and other neighbouring nuclei where many unpaired crossings and numerous aligned oblate states are predicted to occur and where other deformed exotic structures become yrast. The latter include the ultrahigh spin TSD bands, which are just beginning to be explored. However their spins, parities and excitation energies are unknown, very much like the situation for axial superdeformation thirty years ago. A fully consistent picture as to the nature of the nucleus in the ultrahigh spin triaxial world thus remains to be uncovered. In addition it is of fundamental interest, before overwhelming rotational forces cause the nucleus to fission, to determine the limit of discrete nuclear states.

The huge gains in sensitivity and resolving power arising from the development of the next generation gamma-ray tracking arrays together new accelerator developments, assures an extremely promising future for nuclear structure physics. We feel the statement made by Ben and Aage

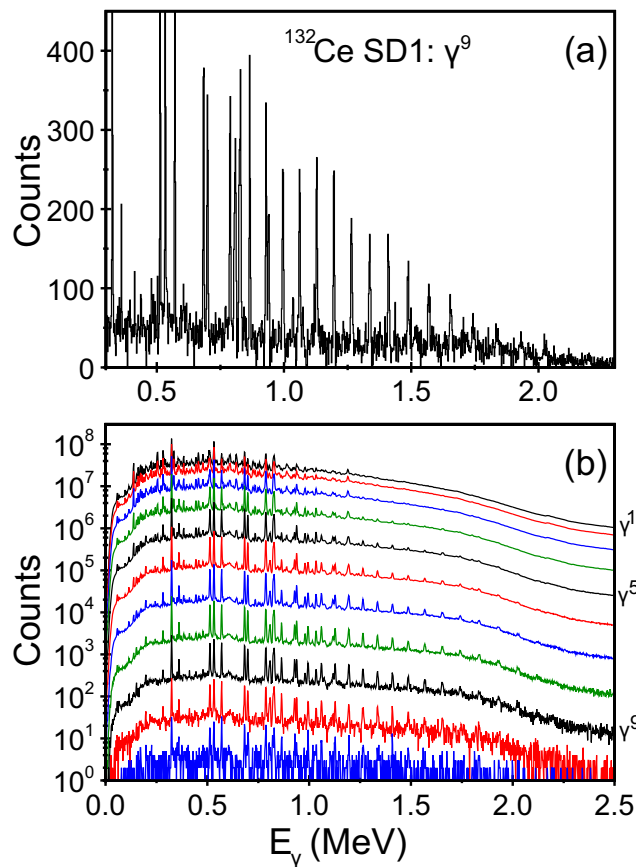


Fig. 24: (a) Gamma-ray spectrum in coincidence with eight simultaneous gating transitions in the yrast highly deformed (SD1) band in ^{132}Ce . The exact spins and excitation energy of this band are still unknown. (b) Various spectra for the band as the coincidence fold for gamma rays is increased from 1 to 11. Taken from our Gammasphere data [123].

“...with the ingenious experimental approaches that are being developed, we may look forward with excitement to the detailed spectroscopic studies that will illuminate the behaviour of the spinning quantized nucleus” is as true today as it was forty years ago!

Acknowledgement

The authors would like to offer their sincere gratitude to Ben and Aage for their remarkable vision and leadership throughout the decades. You have been the true “fathers” of our field and inspired us all. THANK YOU!

We would also like to dedicate this article to Jerry D. Garrett and John C. Lisle who helped pioneer modern nuclear structure studies into the high angular momentum realm of the atomic nucleus. Their wisdom, insight, and brilliance are sadly missed but their joyous spirit and belief in the beauty of the physical world will remain forever in our memories. Two of us (MAR and JS) would also like to especially thank John F. Sharpey-Schafer for introducing them to the rare-earth region and high-resolution gamma-ray spectroscopy. In addition we would like to sincerely thank all our friends involved in collecting and interpreting the data discussed within the present article. It has been, and continues to be, a lot of fun. May the Force always be with you!

This work has been supported in part by the U.S. National

Science Foundation (PHY-1401574), the State of Florida, and the United Kingdom Science and Technology Facilities Council.

References

- [1] Bohr A and Mottelson B R 1975 *Nuclear Structure vol. II* (W.A. Benjamin Inc., New York), and references therein
- [2] Lilley J S 1982 *Physica Scripta* **25** no 3 435
- [3] Bohr N, Kalckar F 1937 *Kgl. Dan. Vid. Selsk. Math. Phys. Medd.* **14** 10
- [4] Riley M A and Simpson J 2013 *Nuclear Gamma Spectroscopy and the Gamma-Spheres*, (*Encyclopaedia of Nuclear Physics and its Applications*, edited by Reinhard Stock, p247-269. Wiley-VCH Publishing, (ISBN 978-3-527-40742-2))
- [5] Lee I Y and Simpson J 2010 *Nucl. Phys. News Intl.* **20** 23
- [6] Lee I Y, Deleplanque M A and Vetter K 2003 *Rep. Prog. Phys.* **66** 1095
- [7] Eberth J and Simpson J 2008 *Progress in Particle and Nuclear Physics* **60** 283
- [8] Beausang C W and Simpson J 1996 *J. Phys. G.* **22** 527-558
- [9] Sharpey-Schafer J F and Simpson J 1988 *Progress in Particle and Nuclear Physics* **21** 293-400
- [10] Nolan P J, Beck F A and Fossan D B 1994 *Ann. Rev. Nuc. Part. Sci.* **44** 561-607
- [11] Simpson J *et al* 1994 *Phys. Lett. B* **327** 187
- [12] Paul E S *et al* 2007 *Phys. Rev. Lett.* **98** 012501
- [13] Wang, X. *et al* 2011 *Phys. Lett. B* **702** 127
- [14] Morinaga H and Gugelot P C 1963 *Nucl. Phys.* **46** 210
- [15] Ryde H *et al* 1973 *Nucl. Phys. A* **207** 513
- [16] Ward D *et al* 1978 *Proc. Canberra Conf., Lecture Notes in Physics*, (Australian Academy of Science) **92** 415
- [17] Riley M A *et al* 1988 *Nucl. Phys. A* **486** 456
- [18] Kondev F G *et al* 1998 *Phys. Lett. B* **437** 35
- [19] Pell E M 1960 *J. Appl. Phys.* **31** 291
- [20] Freck D V and Wakefield J 1960 *Nature* **193** 669
- [21] Tavendale A J and Ewan G T 1963 *Nucl. Instrum. Methods* **25** 125
- [22] Johnson A, Ryde H and Sztarkier J 1971 *Phys. Lett.* **34B** 605
- [23] Riedinger L L *et al* 1980 *Phys. Rev. Lett.* **44** 568

- [24] Bengtsson R and Frauendorf S 1979 *Nucl. Phys.* **A314** 27
- [25] Bengtsson R and Frauendorf S 1979 *Nucl. Phys.* **A327** 139
- [26] Lee I Y 1990 *Nucl. Phys.* **A520** 641c
- [27] Janssens R V F and Stephens F S 1996 *Nucl. Phys. News* **6** 9
- [28] Available at:
<http://nucalf.physics.fsu.edu/riley/gamma/>
- [29] Blons J *et al* 1989 *Nucl. Phys.* **A502** 121c
- [30] Krasznahorkay A *et al* 1998 *Phys.Rev.Lett.* **80** 2073
- [31] Nyako B N *et al* 1986 *Phys. Rev. Lett.* **56** 2680
- [32] Twin P J *et al* 1986 *Phys. Rev. Lett* **57** 811
- [33] Nolan P J *et al* 1985 *J. Phys. G: Nucl. Phys.* **11** L17
- [34] Lauritsen T *et al* 2002 *Phys. Rev. Lett.* **88** 042501
- [35] Strutinsk V M 1967 *Nucl. Phys.* **A95** 420
- [36] Strutinsk V M 1968 *Nucl. Phys.* **A122** 1
- [37] Bjornholm S and Lynn J E 1980 *Rev. Mod. Phys.* **52** 725
- [38] Satula W and Wyss R 2005 *Reports on Progress in Physics* **68** 131
- [39] Nyako B M *et al* 1984 *Phys. Rev. Lett.* **52** 507
- [40] Bentley M A *et al* 1987 *Phys. Rev. Lett.* **59** 2141
- [41] Dagnall P J *et al* 1994 *Phys. Lett.* **B335** 313
- [42] Lauritsen T *et al* 2002 *Phys. Rev. Lett.* **89** 282501
- [43] Lauritsen T *et al* 2007 *Phys. Rev. C.* **75** 064309
- [44] Kirwan A J *et al* 1987 *Phys. Rev. Lett.* **58** 467
- [45] Moore E F *et al* 1989 *Phys Rev Lett* **63** 360
- [46] Riley M A *et al* 1990 *Nucl. Phys.* **A** 512 178
- [47] Cullen D M *et al* 1990 *Phys. Rev. Lett.* **65** 1547
- [48] Nolan P J and Twin P J 1988 *Ann. Rev. Nucl. Part. Sci.* **38** 533
- [49] Sharpey-Schafer J F and Simpson J, 1988 *Prog. in Part. Nucl. Phys.*, 21 293
- [50] Åberg S, Flocard H, and Nazarewicz W, 1990 *Ann. Rev. Nucl. Part. Sci.*, 40 439
- [51] Janssens R V F and Khoo T L 1991 *Ann. Rev. Nucl. Part. Sci.* **41** 321
- [52] Singh B, R.B. Firestone R B and Chu S Y F 1996 it Table of Superdeformed Nuclear Bands and Fission Isomers, Second Edition *Nucl. Data Sheets* **781**
- [53] Byrski T *et al* 1990 *Phys. Rev. Lett.* **64**, 1650
- [54] Nazarewicz W, Twin P J, Fallon P, and Garrett J D 1990 *Phys. Rev. Lett.* **64** 1654
- [55] Stephens F S *et al* 1990 *Phys. Rev. Lett.* **64** 2623
- [56] Stephens F S *et al* 1990 *Phys. Rev. Lett.* **65** 301
- [57] Fallon P, Nazarewicz N, Riley M A, and Wyss R 1992 *Phys. Lett.* **B** 276 427
- [58] Joyce M J *et al* 1993 *Phys. Rev. Lett.* **71** 2176
- [59] Baktash C, Haas B, and Nazarewicz W 1995 *Annu. Rev. Nucl. Part. Sci.* **45** 485
- [60] Fallon P *et al* 1999 *Phys. Rev.* **C60** 044301
- [61] Flibotte S *et al* 1993 *Phys. Rev. Lett.* **71** 4299
- [62] Haslip D S *et al* 1998 *Phys. Rev.* **C57** 2196
- [63] Haslip D S, Flibotte S, Svensson C E and Waddington J C 1998 *Phys. Rev.* **C58** R1889
- [64] Ward D, Waddington J C, and Svensson C E 2016 *Phys. Scripta* **91** 033002
- [65] Szymanski Z 1983 *Fast Nuclear Rotation* (Clarendon Press, Oxford, England)
- [66] Ring P and Schuck P 1980 *The Nuclear Many-Body Problem* (Springer-Verlag, Heidelberg)
- [67] Krane K S 1988 *Introductory Nuclear Physics* (John Wiley and Sons, New York)
- [68] Ejiri H and de Voigt M J A 1989 *Gamma-Ray and Electron Spectroscopy in Nuclear Physics* (Clarendon Press)
- [69] Nilsson S G, Ragnarsson I 1995 *Shapes and Shells in Nuclear Structure* (Cambridge University Press, Cambridge, England)
- [70] Heyde K 1999 *Basic Ideas and Concepts in Nuclear Physics* (Institute of Physics, Bristol)
- [71] Pancholi S C 2011 *Exotic Nuclear Excitations* (New York: London: Springer, - Springer tracts in modern physics)
- [72] Casten R F 2001 *Nuclear Structure from a Simple Perspective* (Oxford Studies in Nuclear Physics, Oxford University Press; 2 edition)
- [73] Wang X, Riley M A, Paul E S and Simpson J 2013 *McGraw-Hill Yearbook of Science and Technology* (McGraw-Hill, 2013)
- [74] Bengtsson T 1990 *Nucl. Phys.* **A512** 124
- [75] Stephens F S and Simons R S 1972 *Nucl. Phys.* **A** **183** 257
- [76] Riley M A and Pipidis P available at:
<http://www.physics.fsu.edu/TheBackBender>
- [77] *Fifty Years of Nuclear BCS* 2013 (Edited by Ricardo A. Broglia and Vladimir Zelevinsky, published by World Scientific, January 2013)

- [78] Beuscher H *et al* 1972 *Phys. Lett.* **B 40** 449
- [79] Lee I Y *et al* 1977 *Phys. Rev. Lett.* **38** 1454
- [80] Burde J *et al* 1982 *Phys. Rev. Lett.* **48**, 530
- [81] Simpson J *et al* 1984 *Phys. Rev. Lett.* **53**, 648
- [82] Tjom P *et al* 1985 *Phys. Rev. Lett.* **55** 2405
- [83] Simpson J *et al* 1994 *Phys. Lett.***B 327** 187
- [84] Ragnarsson I, Xing Z, Bengtsson T, Riley M A 1986 *Phys. Scr.* **34** 651
- [85] Pipidis P 2006 *Ph.D. thesis* Florida State University
- [86] Evans A O *et al* 2004 *Phys. Rev. Lett.* **92** 252502
- [87] Evans A O *et al* 2006 *Phys. Rev. C* **73** 064303
- [88] Paul E S *et al* *Phys. Rev. Lett.* **98** 012501
- [89] Odegard S W *et al* 2001 *Phys. Rev. Lett.* **86** 5866
- [90] Hartley D J *et al* 2005 *Phys. Lett.* **B 608** 31
- [91] Bengtsson T and Ragnarsson I 1983 *Physica Scripta* **T5** 165
- [92] Dudek J and Nazarewicz W 1985 *Phys. Rev. C* **31** 298
- [93] Jensen D R *et al* 2002 *Phys. Rev. Lett.* **89** 142503
- [94] Anderson G *et al* 1976 *Nucl. Phys.* **A 268** 205
- [95] Carlsson B G *et al* 2008 *Phys. Rev. C* **78** 034316
- [96] Wang X *et al* 2011 *Phys. Lett.* **B 702** 127
- [97] Wang X *et al* 2012 *J. Phys. Conf. Ser.* **381** 012065
- [98] Shepherd S L *et al* 2002 *Phys. Rev. C* **65** 034320
- [99] Carlsson B G and Ragnarsson I 2006 *Phys. Rev. C* **65** 011302(R)
- [100] Revill J P *et al* 2012 *J. Phys. Conf. Ser.* **381** 012066
- [101] Nisius D N *et al* 1997 *Phys. Lett.* **B 392** 18
- [102] Frauendorf S 2001 *Rev. Mod. Phys.* **73** 463
- [103] Shi Y *et al* 2012 *Phys. Rev. Lett.* **108** 092501
- [104] Shi Y, Zhang C L, Dobaczewski J, and Nazarewicz W 2013 *Phys. Rev. C* **88** 034311
- [105] Kardan A, Ragnarsson I, Miri-Hakimabad H and Rafat-Motevali L 2012 *Phys. Rev. C* **86**, 014309
- [106] Afanasjev A V, Shi Y, Nazarewicz W, 2012 *Phys. Rev. C* **86**, 031304(R)
- [107] Lagergren K *et al.* 2001 *Phys. Rev. Lett.* **87** 022502
- [108] Teal C *et al.* 2008 *Phys. Rev. C* **78** 017305
- [109] Ollier J *et al.* 2009 *Phys. Rev. C* **80** 064322
- [110] Aguilar A *et al.* 2008 *Phys. Rev. C* **77** 021302(R)
- [111] Hartley D J *et al* 2009 *Phys. Rev. C* **80**, 041304(R)
- [112] Riley M A, Garrett J D, Simpson J, Sharpey-Schafer J F 1988 *Phys. Rev. Lett.***60** 553
- [113] Riley M A *et al* 1990 *J. Phys. G: Nucl. Part. Phys.* **16** L67
- [114] Kondev F G *et al* 1999 *J. Phys. G: Nucl. Part. Phys.* **25** 897
- [115] Simpson J *et al* 2000 *Phys. Rev. C* **62** 024321
- [116] Ragnarsson I and Bengtsson T 1985 *Nucl. Phys.* **A 447** 251
- [117] Morrison J D *et al* 1998 *Europhys. Lett.* **6(6)** 493
- [118] Afanasjev A V, Fossan D B, Lane G J, Ragnarsson I 1999 *Phys. Rep.* **322** 1
- [119] Janzen V P *et al* 1994 *Phys. Rev. Lett.* **72** 1160
- [120] Ragnarsson I, Janzens V P, Fossan D B Schmeing N C and Wadsworth R 1995 *Phys. Rev. Lett.* **74** 3935.
- [121] Afanasjev A V and Ragnarsson I 1996 *Nucl. Phys.* **A 608** 176
- [122] Paul E S *et al* 2005 *Phys. Rev. C* **71** 054309.
- [123] Paul E S *et al* *to be published*